

Nitrogen Oxide Concentrations in Natural Waters on Early Earth

Sukrit Ranjan^{1,*}, Zoe R. Todd², Paul B. Rimmer^{3,4}, Dimitar D. Sasselov²,
Andrew R. Babbitt¹

¹Massachusetts Institute of Technology, Department of Earth, Atmospheric, and Planetary Sciences

²Harvard University, Department of Astronomy

³MRC Laboratory of Molecular Biology

⁴University of Cambridge, Cavendish Astrophysics

¹77 Massachusetts Avenue, Cambridge, MA 02139

²60 Garden Street, Cambridge, MA 02138

³Francis Crick Ave, Cambridge CB2 0QH, UK

⁴JJ Thomson Avenue, Cambridge CB3 0HE, UK

Key Points:

- Nitrate and nitrite (NO_X^-) are relevant to prebiotic chemistry. Past work has argued these molecules were abundant in the early ocean.
- Fe^{2+} and UV suppress $[\text{NO}_X^-]$ to much lower concentrations than previously thought in the ocean. $[\text{NO}_X^-]$ could have been higher in ponds.
- Most NO_X^- should have been nitrate. Prebiotic chemistries that use nitrate are more plausible than those that use nitrite.

arXiv:1902.07740v1 [astro-ph.EP] 20 Feb 2019

Corresponding author: Sukrit Ranjan, Email: sukrit@mit.edu. T: 617-253-6283. F: 617-324-2055. Mailing: 77 Massachusetts Avenue, Room 54-1719, Cambridge, MA 02139

Abstract

A key challenge in origins-of-life studies is estimating the abundances of species relevant to the chemical pathways proposed to have contributed to the emergence of life on early Earth. Dissolved nitrogen oxide anions (NO_x^-), in particular nitrate (NO_3^-) and nitrite (NO_2^-), have been invoked in diverse origins-of-life chemistry, from the oligomerization of RNA to the emergence of protometabolism. Recent work has calculated the supply of NO_x^- from the prebiotic atmosphere to the ocean, and reported steady-state $[\text{NO}_x^-]$ to be high across all plausible parameter space. These findings rest on the assumption that NO_x^- is stable in natural waters unless processed at a hydrothermal vent. Here, we show that NO_x^- is unstable in the reducing environment of early Earth. Sinks due to UV photolysis and reactions with reduced iron (Fe^{2+}) suppress $[\text{NO}_x^-]$ by several orders of magnitude relative to past predictions. For $\text{pH} = 6.5 - 8$ and $T = 0 - 50^\circ\text{C}$, we find that it is most probable that $[\text{NO}_x^-] < 1 \mu\text{M}$ in the prebiotic ocean. On the other hand, prebiotic ponds with favorable drainage characteristics may have sustained $[\text{NO}_x^-] \geq 1 \mu\text{M}$. As on modern Earth, most NO_x^- on prebiotic Earth should have been present as NO_3^- , due to its much greater stability. These findings inform the kind of prebiotic chemistries that would have been possible on early Earth. We discuss the implications for proposed prebiotic chemistries, and highlight the need for further studies of NO_x^- kinetics to reduce the considerable uncertainties in predicting $[\text{NO}_x^-]$ on early Earth.

1 Introduction

A key challenge for origin-of-life studies is determining the range of environmental conditions on early Earth under which life arose. Knowledge of these environmental conditions informs development of theories of the origin of life, and enables assessment of the plausibility and probability of postulated prebiotic chemistries (e.g., Bada, Bigham, and Miller (1994); Corliss, Baross, and Hoffman (1981); Ruiz-Mirazo, Briones, and de la Escosura (2014); Todd et al. (2018); Urey (1952); Xu et al. (2018)). Consequently, extensive work has been done to place constraints on the prebiotic environment, including but not limited to the availability of liquid water, the redox state of the atmosphere, the UV irradiation environment, the pH and temperature of the early oceans, the physico-chemical conditions at deep-sea hydrothermal vents, and the availability of sulfidic anions (Farquhar, Bao, & Thiemens, 2000; Halevy & Bachan, 2017; Krissansen-Totton, Arney, & Catling, 2018; Martin, Baross, Kelley, & Russell, 2008; Mojzsis, Harrison, & Pidgeon, 2001; Ranjan & Sasselov, 2017; Ranjan, Todd, Sutherland, & Sasselov, 2018).

An important prebiotic environmental factor is the abundance of fixed nitrogen species in natural waters on early Earth. Dinitrogen's high-energy triple bond renders it highly nonreactive, meaning that nitrogen generally must be "fixed" into its reduced or oxidized forms (e.g., NO_2^- , NO_3^- , NH_4^+) to be useful to biology or prebiotic chemistry. Consequently, it is unsurprising that nitrogen fixation is thought to be ancient (Canfield, Glazer, & Falkowski, 2010; Fani, Gallo, & Lio, 2000; Stüeken, Buick, Guy, & Koehler, 2015; Zehr & Ward, 2002; Zerkle & Mikhail, 2017). Prebiotic chemists have been especially interested in nitrate (NO_3^-) and nitrite (NO_2^-), the oxidized anions of nitrogen (NO_x^-). These molecules are high-potential electron acceptors, have played a key role in microbial metabolisms since at least the Archaean (Canfield et al., 2010), and have been hypothesized to have been involved in the first metabolic pathways, e.g. the oxidation of methane and hydrogenation of CO_2 at deep-sea vents (Ducluzeau et al., 2009; Nitschke & Russell, 2013; Shibuya, Russell, & Takai, 2016). These molecules have also been invoked for the non-enzymatic synthesis and replication of oligonucleotides, in surficial (lake/pond) settings (Mariani, Russell, Javelle, & Sutherland, 2018). Crucially, NO_x^- can be abiotically synthesized by the thermal decay of molecules like HNO, which are produced by high-energy events like lightning in an $\text{N}_2\text{-CO}_2$ atmosphere (Ardaseva et al., 2017;

Kasting & Walker, 1981; Mancinelli & McKay, 1988; Navarro-González, Molina, & Molina, 1998), meaning these molecules may have been available for prebiotic chemistry on early Earth.

Motivated by the potential prebiotic relevance of NO_3^- and NO_2^- , a number of studies have aimed to constrain their concentrations on early Earth. Mancinelli and McKay (1988) pointed out that atmospherically-generated NO_x^- would form NO_2^- and NO_3^- in the prebiotic ocean and accumulate, and that solubility concerns would not limit the accumulation. However, Mancinelli and McKay (1988) did not quantify the concentrations to which NO_x^- could accumulate. Wong, Charnay, Gao, Yung, and Russell (2017) conducted atmospheric modeling, combining 3D General Circulation Model (GCM) estimates with 1D photochemical models to estimate the supply of NO_x^- to the oceans due to lightning. They identified the key variable controlling the NO_x^- supply to be the CO_2 partial pressure ($p\text{CO}_2$). Under the assumption that the sole sink on NO_x^- was destruction at high-temperature hydrothermal vents, Wong et al. (2017) computed $[\text{NO}_x^-]$ in the bulk ocean to be $\geq 10\mu\text{M}$, and $[\text{NO}_x^-] = 20\text{ mM}$ for $p\text{CO}_2 = 1\text{ bar}$. Laneuville, Kameya, and Cleaves (2018) conducted a systems model of the prebiotic nitrogen cycle, including cometary delivery, impact synthesis, and lightning as sources of fixed nitrogen, and destruction at hydrothermal vents as the sole sink of oceanic NO_x^- . They calculated $[\text{NO}_x^-] \approx 1\mu\text{M} - 10\text{mM}$ in the bulk prebiotic oceans, depending on a number of variables including atmospheric nitrogen fixation rate. These large ranges are due to the wide range of possible NO_x^- supply. Both Wong et al. (2017) and Laneuville et al. (2018) suggest that the prebiotic oceans should have had $\geq 1\mu\text{M}$ $[\text{NO}_x^-]$, thought to be adequate for prebiotic chemistry. For comparison, on modern earth, bioavailable fixed NO_x^- achieves maximum concentrations of $\sim 40\mu\text{M}$ in the deep Pacific (Olsen et al., 2016; Zehr & Ward, 2002). NO_x^- in the modern ocean is almost exclusively in the form of NO_3^- , except where NO_2^- accumulates substantially within two depth horizons. The primary nitrite maximum, where nitrite concentrations reach hundreds of nanomolar to occasionally a few micromolar, is a global feature at the base of the photic zone, and formed by leaking algal cells (Lomas & Lipschultz, 2006) and/or an imbalance in the ammonium and nitrite oxidation steps of nitrification (Santoro et al., 2013). The secondary nitrite maximum is a broad feature in the oxygen deficient zones of the eastern tropical Pacific and Arabian Sea, where oxygen levels are reduced to $< 10\text{ nmol/L}$ (Revsbech et al., 2009). These secondary nitrite maxima can achieve several micromolar in concentration (e.g., Babbín, Keil, Devol, and Ward 2014) and are indicative of active denitrification regimes.

Overall, previous work has concluded that high $[\text{NO}_x^-]$ (micromolar to millimolar) was present in the prebiotic ocean, under the assumption that the only sink of NO_x^- in the prebiotic ocean was processing at hydrothermal vents, and that atmospherically-supplied NO_x^- was otherwise stable in prebiotic waters. However, in the anoxic prebiotic environment, NO_2^- and NO_3^- are vulnerable to reduction to less soluble forms due to UV photochemistry and reactions with reductants (e.g., Fe^{2+}). These reduced species (NO , N_2O , N_2) can then escape to the atmosphere, depleting the oceanic nitrogen pool (Carpenter & Nightingale, 2015).

In this paper, we explore the impact of these chemical sinks on the predicted concentrations of NO_x^- in prebiotic waters. In Section 2, we carry out a kinetic calculation, comparing the supply of NO_x^- to natural waters to the sinks of NO_x^- from reduction reactions and photochemistry to estimate the steady-state concentration of NO_x^- in oceans and ponds with $T = 0 - 50^\circ\text{C}$ and $\text{pH} = 6.5 - 8$. In Section 3, we examine the thermochemical stability of NO_3^- and NO_2^- in prebiotic conditions, finding results consistent with our kinetic calculations. In Section 4, we discuss our calculations and explore their implications for prebiotic NO_x^- levels, postulated prebiotic chemistries, and origin-of-life scenarios. We summarize our conclusions in Section 5.

2 Kinetic Steady-State

In this section, we calculate abiotic loss of aqueous NO_2^- and NO_3^- due to reduction by UV light and Fe^{2+} , and compare to the NO_X^- supply rate from processes such as lightning fixation and exogenous delivery, to estimate steady-state NO_X^- concentrations. We focus on these processes because they are dominant under the range of conditions available on early Earth. If abiotic NO_X^- destruction is slow compared to abiotic NO_X^- production, then it is possible for high levels of NO_X^- to build up in natural waters. If destruction is fast compared to production, then NO_X^- levels will be low.

2.1 NO_X^- Production

On modern Earth, lightning fixation is the largest non-biological natural source of fixed nitrogen, via high-energy shocks which form free radicals and disrupt N_2 (Mancinelli & McKay, 1988). Wong et al. (2017) used photochemical models calibrated with GCM results to model the supply of NO_X^- to the prebiotic surface due to lightning fixation. Most NO_X^- reached the surface in the form of HNO , which in aqueous settings would then undergo dissociation, homologation, and decay reactions, ultimately yielding soluble NO_2^- and NO_3^- , and gaseous N_2O (Mancinelli & McKay, 1988; Summers & Khare, 2007). Stanton et al. (2018) have recently demonstrated the reduction of NO to N_2O in ferrous waters; we may speculate similar chemodenitrification to occur with NO^- . It is difficult to calculate the fraction of fixed nitrogen that escapes back to the atmosphere as N_2O , because the kinetics of these transformations have not been quantified for NO^- . We follow Wong et al. (2017) in neglecting the sink to N_2O formation and assuming all NO_X^- supplied to the surface from the atmosphere eventually yields NO_2^- and/or NO_3^- ; this means our calculations may overestimate NO_X^- supply and hence $[\text{NO}_X^-]$. Wong et al. (2017) report a dominant factor controlling the surface flux of NO_X^- to be the partial pressure of CO_2 in the atmosphere; the minimum NO_X^- flux, $\phi_{\text{NO}_X^-}$, was $\phi_{\text{NO}_X^-} = 2.5 \times 10^5 \text{ cm}^{-2} \text{ s}^{-1}$ for $\text{pCO}_2 = 0.1 \text{ bar}$, and the maximum was $\phi_{\text{NO}_X^-} = 6.5 \times 10^8 \text{ cm}^{-2} \text{ s}^{-1}$ for $\text{pCO}_2 = 1 \text{ bar}$.

We used the lightning atmospheric chemistry model from Ardaseva et al. (2017) to explore the production of NO_X^- by lightning as a function of pN_2 , pCO_2 , and lightning flash rate, to verify the upper bound in NO_X^- production rate identified by Wong et al. (2017). This model uses the freeze-out temperature approximation; a more sophisticated approach would involve shock modeling. We compare our lightning model calculations to the experimental results tabulated in Mvondo, Navarro-González, McKay, Coll, and Raulin (2001), and find we reproduce these results well for CO_2 mixing ratios $\gtrsim 0.2$; at lower CO_2 concentrations, we overpredict NO_X^- production. We therefore only apply our model to atmospheres with CO_2 mixing ratios ≥ 0.2 .

We find NO_X^- production to be strong functions of pN_2/pCO_2 and pCO_2 . NO_X^- production decreases as pN_2/pCO_2 increases, because the probability of N atoms recombining to N_2 is higher (as opposed to reacting with CO_2 -derived oxygen to form NO_X^-). We find NO_X^- production increases with pCO_2 over the range $\text{pCO}_2 = 0.1 - 10 \text{ bar}$. This contrasts to Wong et al. (2017), who report a maximum in NO_X^- production at $\text{pCO}_2 = 1 \text{ bar}$; this is because Wong et al. (2017) calculate lower lightning flash rates for high pCO_2 due to lack of moist convection in the warm troposphere they calculate for $\text{pCO}_2 = 10 \text{ bar}$, while we fix the lightning flash rate. If we extrapolate the finding of Marty, Zimmermann, Pujol, Burgess, and Philippot (2013) that $\text{pCO}_2 \leq 0.7 \text{ bar}$ and $\text{pN}_2 \geq 0.5 \text{ bar}$ from 3-3.5 Ga to the prebiotic era (c. 3.9 Ga) and assume lightning energies and flash densities similar to modern Earth, we find a tropospheric NO_X^- production rate of $\phi_{\text{NO}_X^-} < 10^9 \text{ cm}^{-2} \text{ s}^{-1}$, in concordance with Wong et al. (2017). Biological fixation tends to decrease pN_2 , suggesting that pN_2 was not lower in the prebiotic era than in the Archaean (Johnson & Goldblatt, 2017). Krissansen-Totton, Olson, and Catling (2018) calculate that weathering restricted $\text{pCO}_2 \leq 1 \text{ bar}$ at 4 Ga. We consequently retain $6.5 \times 10^8 \text{ cm}^{-2} \text{ s}^{-1}$

of Wong et al. (2017) as the upper bound on $\phi_{NO_X^-}$, but caution that if pCO_2 were higher or pN_2 lower than what we consider, $\phi_{NO_X^-}$ could have been up to an order of magnitude higher. For more details, see SI Section S4.

Comet delivery and impact fixation should also have supplied fixed nitrogen on prebiotic Earth; however, these mechanisms are thought to have supplied $\phi_{NO_X^-} < 2 \times 10^9 \text{ cm}^{-2} \text{ s}^{-1}$ and typically less, well within the range bracketed by lightning production (Laneuville et al., 2018). Airapetian, Gloer, Gronoff, Hébrard, and Danchi (2016) suggest that energetic protons from flares on the young Sun might also have powered nitrogen fixation and the supply of NO_X^- to the surface; however, they do not quantify the magnitude of this supply. We consequently focus on the NO_X^- production flux range defined by lightning production in the model of Wong et al. (2017) in our work ($2.5 \times 10^5 - 6.5 \times 10^8 \text{ cm}^{-2} \text{ s}^{-1}$).

2.2 NO_X^- Destruction

We consider three processes in calculating NO_X^- destruction in natural waters: processing at hydrothermal vents, UV photolysis, and reactions with Fe^{2+} . Past work has focused on processing at vents; in this work, we consider the effects of UV and Fe^{2+} as well. SI Section S5 explores these processes in detail, along with other NO_X^- loss processes we neglected in this work because they are dominated by the processes we consider here.

The presence of UV light on early Earth is attested to by the sulfur mass-independent fractionation (SMIF) signal (Farquhar, Savarino, Airieau, & Thiemens, 2001). The presence of Fe^{2+} is attested by the presence of banded iron formations (BIFs) and other geological evidence (Cloud, 1973; Klein, 2005; Li et al., 2013; Walker & Brimblecombe, 1985). Recent estimates place $[Fe^{2+}] = 30 - 600 \mu\text{M}$ in early Archean oceans, with higher $[Fe^{2+}]$ in the aphotic deep oceans (Halevy & Bachan, 2017; Konhauser et al., 2017; Tosca, Guggenheim, & Pufahl, 2016; Zheng, Beard, Roden, Czaja, & Johnson, 2018). In this work, we explore $[Fe^{2+}] = 10 - 600 \mu\text{M}$, bracketing this range. We do not consider reactions with other reductants, such as Mn^{2+} , owing to paucity of constraints on the kinetics of these processes; consequently, we may underestimate NO_X^- reduction rates in prebiotic natural waters.

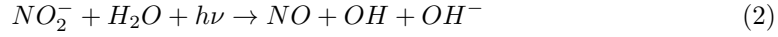
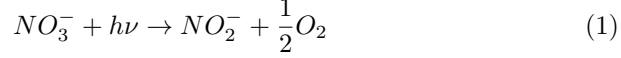
The rates of NO_X^- photolysis by UV and reduction by Fe^{2+} are dependent on temperature and pH. In this work, we consider $\text{pH} = 6.5 - 8$ and $T = 273 - 323 \text{ K}$, motivated by modeling work which predicts the early ocean to have been circumneutral ($6.3 \leq \text{pH} \leq 7.2$) and temperate ($271 \leq T \leq 314 \text{ K}$) (Krissansen-Totton et al. (2018); see also Halevy and Bachan (2017)). We consider the sensitivity of our conclusions to these assumptions in Section 2.4.

2.2.1 NO_X^- Destruction in Vents

The hot and acidic conditions at hydrothermal vents can destroy NO_X^- (Brandes et al., 1998; R ay, Dey, & Ghosh, 1917; Summers, 2005). It is debated how extreme conditions need to be to consume NO_X^- . Under the assumptions that NO_X^- is removed with unit efficiency at and only at black smoker-type vents ($T \lesssim 405^\circ \text{ C}$, $\text{pH} = 1 - 2$, Martin et al. (2008)), Wong et al. (2017) propose NO_X^- destruction to be characterized by a first-order process with rate constant $k_{vents} = 8 \times 10^{-17} \text{ s}^{-1}$. Under the assumption that circulation through any hydrothermal vent would destroy 100% of NO_X^- , Laneuville et al. (2018) instead propose $k_{vents} = 1 \times 10^{-14} \text{ s}^{-1}$. We explore the range $k_{vents} = 8 \times 10^{-17} - 1 \times 10^{-14} \text{ s}^{-1}$ in this work.

2.2.2 NO_X^- Destruction by UV

Irradiation by UV light in natural waters net photolyzes NO_3^- to NO_2^- , and NO_2^- to NO, which escapes the ocean to the atmosphere or is reduced to N_2O (Carpenter & Nightingale, 2015; Fanning, 2000; Mack & Bolton, 1999; Spokes & Liss, 1996; Stanton et al., 2018):



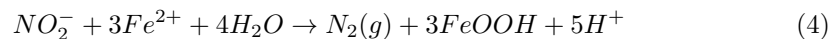
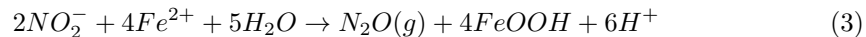
These processes are thought to be first order and have been measured both in the oceans and in lakes. In the modern surface ocean, these processes have median rate constants $k_{\text{NO}_3^-,h\nu} = 2.3 \times 10^{-8} \text{ s}^{-1}$ and $k_{\text{NO}_2^-,h\nu} = 1.2 \times 10^{-6} \text{ s}^{-1}$ for nitrate and nitrite, respectively (Minero et al., 2007; Zafriou & True, 1979a, 1979b). In pure water, NO_2^- reacts with OH to reform NO_3^- ; however, in the presence of OH scavengers like bicarbonate or Br^- , NO_2^- is lost with 20-100% efficiency (Treinin & Hayon, 1970; Zafriou, 1974; Zafriou, Jousset-Dubien, Zepp, & Zika, 1984; Zafriou & True, 1979b).

Nitrite and nitrite photolysis rates, as measured by OH production, depend modestly on temperature. At $T = 0^\circ \text{ C}$, photolysis rates are $\geq 0.5 \times$ the rates at $T = 25^\circ \text{ C}$, and at $T = 50^\circ \text{ C}$, photolysis rates are $\leq 2 \times$ the rates at $T = 25^\circ \text{ C}$ (Mack & Bolton, 1999; Zellner, Exner, & Herrmann, 1990). The reaction rates measured by Zafriou and True (1979b) and Zafriou and True (1979a) were measured at ambient temperature. Under the assumption that these ambient conditions corresponded to $T \approx 25^\circ \text{ C}$, we explore $k_{\text{NO}_3^-,h\nu} = 1.1 - 4.6 \times 10^{-8} \text{ s}^{-1}$ and $k_{\text{NO}_2^-,h\nu} = 0.6 - 2.4 \times 10^{-6} \text{ s}^{-1}$, to account for the variation in photolysis rates with temperature for $T = 0 - 50^\circ \text{ C}$.

We calculate the global rate of nitrate/nitrite photolysis following a procedure motivated by that of Zafriou and True (1979a) and Zafriou and True (1979b). We assume that nitrate and nitrite are lost at rates equal to half their surface photolysis rates down to their photic depths, and that the loss rates are zero below this threshold. The modern photic depth for nitrate and nitrite at the equator are 5 m and 10 m, respectively; to average over latitude and obtain global mean photic depths, we scale these photic depths by 2/3 (Cronin, 2014; Zafriou & True, 1979a, 1979b). In the modern ocean, intense consumption by phototrophic microbes depletes surficial NO_X^- , meaning that NO_X^- photolysis is only significant in upwelling areas where NO_X^- is maintained at high concentrations due to supply from below. In the absence of biology, surface NO_X^- would not be depleted, and NO_X^- would be photolyzed from 100% of the surface area of the ocean. When calculating the loss of NO_X^- in pond and lake environments, we assume the same photic depths, and continue to take NO_X^- to be lost from 100% of the surface area. We neglect possible enhancements in the conversion rate due to factors such as availability of shorter-wavelength UV radiation on early Earth and the anoxic nature of prebiotic natural waters, and we assume the lowest proposed efficiency for net loss of NO_2^- to photolysis (i.e., 20%). Consequently, our estimates of NO_X^- photolysis should be considered lower bounds.

2.2.3 Reduction of NO_2^- by Fe^{2+} to Nitrogenous Gas

Fe^{2+} reduces NO_2^- to yield nitrogenous gas (Buchwald, Grabb, Hansel, & Wankel, 2016):



Recent kinetic studies of these reactions are consistent with first-order kinetics with respect to both reactants and second order kinetics overall, with rate constants that are

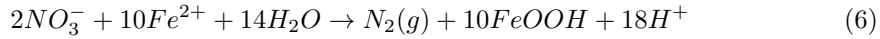
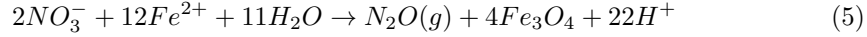
dependent on pH (Buchwald et al., 2016; Grabb, Buchwald, Hansel, & Wankel, 2017; Jones, Peters, Lezama Pacheco, Casciotti, & Fendorf, 2015). From the data of Buchwald et al. (2016) and Grabb et al. (2017), we extract $k_{NO_2^-, Fe^{2+}} = 3 \times 10^{-5} - 1 \times 10^{-2} \text{ M}^{-1} \text{ s}^{-1}$ over pH=6.5-8 and T= 25° C (SI Section S5).

$k_{NO_2^-, Fe^{2+}}$ depends on whether Fe^{2+} or NO_2^- is in excess, with reaction rates up to an order of magnitude lower if $[NO_2^-] > [Fe^{2+}]$ compared to if $[NO_2^-] < [Fe^{2+}]$ (Jones et al., 2015). To account for the potential dependence on relative NO_2^- and Fe^{2+} concentrations, we assign $k_{NO_2^-, Fe^{2+}}([NO_2^-] > [Fe^{2+}]) = 0.1k_{NO_2^-, Fe^{2+}}([NO_2^-] < [Fe^{2+}])$. Further, The activation energy E_A for NO_2^- reduction by dissolved Fe^{2+} has not been measured to our knowledge, but is 18.4 kJ mol⁻¹ for NO_2^- reduction by mineralized Fe^{2+} , and is 70 kJ mol⁻¹ for NO_3^- reduction by dissolved Fe^{2+} (Ottley, Davison, & Edmunds, 1997; Samarkin et al., 2010). Mineralized Fe^{2+} is a more effective reductant than dissolved Fe^{2+} , and NO_2^- is more reactive than NO_3^- , suggesting $18.4 \leq E_A \leq 70 \text{ kJ mol}^{-1}$. To ensure we do not underestimate the possible range of $k_{NO_2^-, Fe^{2+}}$, we take $E_A = 70 \text{ kJ mol}^{-1}$.

Combining these effects, in total we consider $k_{NO_2^-, Fe^{2+}} = 2 \times 10^{-6} - 9 \times 10^{-2} \text{ M}^{-1} \text{ s}^{-1}$ if $[NO_2^-] < [Fe^{2+}]$ and $k_{NO_2^-, Fe^{2+}} = 2 \times 10^{-7} - 9 \times 10^{-3} \text{ M}^{-1} \text{ s}^{-1}$ if $[NO_2^-] > [Fe^{2+}]$, corresponding to pH= 6.5 - 8 and $T = 0 - 50^\circ \text{ C}$.

2.2.4 Reduction of NO_3^- by Fe^{2+} to Nitrogenous Gas

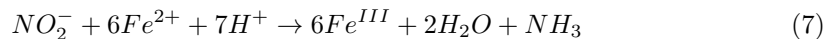
Fe^{2+} can reduce NO_3^- to nitrogenous gas, with proposed reactions (Postma, 1990; Samarkin et al., 2010):



The kinetics of uncatalyzed room-temperature reduction of NO_3^- by Fe^{2+} at room temperature are uncertain, because NO_3^- reduction is very slow under these conditions and hence difficult to characterize in the laboratory. Ottley et al. (1997) reports the detection of uncatalyzed NO_3^- reduction by Fe^{2+} at room temperature over timescales of a week. However, Picardal (2012) report nondetections of NO_3^- reduction by Fe^{2+} in sterile incubations carried out under conditions and timescales similar to those of Ottley et al. (1997). As we are unable to favor one study above the other from available information, we consider a range of $k_{NO_3^-, Fe^{2+}} = 0 - 9 \times 10^{-4} \text{ M}^{-1} \text{ s}^{-1}$. The lower bound is derived from the reported nondetections of Picardal (2012). The upper bound is derived from the study of Ottley et al. (1997), and corresponds to pH= 8 and $T = 50^\circ \text{ C}$, which should be the maximum rate possible over pH= 6.2 - 9 and $T = 0 - 50^\circ \text{ C}$ (Petersen, 1979). We assume that the reduction of NO_3^- by dissolved Fe^{2+} is, like the reduction of NO_2^- , first-order with respect to both reactants, for a second-order reaction overall, motivated by the generally similar kinetics of NO_2^- and NO_3^- reduction by $Fe(0)$, H_2 , and mineralized Fe^{2+} (Samarkin et al., 2010; Zhu & Getting, 2012). This range of $k_{NO_3^-, Fe^{2+}}$ is very large; kinetic studies are required to constrain it.

2.2.5 Other Reactions of NO_X^- with Fe^{2+}

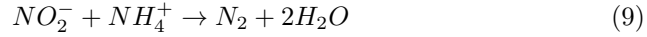
Fe^{2+} can also reduce NO_2^- to NH_3 , with proposed empirical reaction mechanism and rate law (Summers & Chang, 1993):



$$\frac{d[NH_3]}{dt} = k_7[NO_2^-][Fe^{2+}]^{1.8} (pH = 7.9) \quad (8)$$

This reaction should be a negligible sink on $[\text{NO}_2^-]$ compared to Fe^{2+} reduction of NO_x^- to nitrogenous gas; to demonstrate this, we evaluate it for $k_7 = 4.2 \times 10^{-5} \text{ s}^{-1} \text{ M}^{-1.8}$, corresponding to the maximum rate (pH= 7.6, $T = 40^\circ\text{C}$) measured by Summers and Chang (1993). UV photolysis and reduction by Fe^{2+} dominate this process over the $[\text{NO}_2^-]$ range we consider here (Figure 1).

Similarly, the anaerobic ammonium oxidation by NO_2^- (anammox) to N_2 is negligible compared to other processes; to illustrate this, we compute its rate for $[\text{NH}_3] = 6 \times 10^{-7} \text{ M}$ and pH= 6.5, $T = 50^\circ \text{ C}$, corresponding to conditions maximize the reaction rate while conforming to the constraints Kasting (1982) and Krissansen-Totton et al. (2018). We take the rate law from Nguyen, Iwaniw, and Fogler (2003) following Lagneville et al. (2018):



$$\frac{d[\text{N}_2]}{dt} = A \exp(-E/RT) [\text{NH}_3] [\text{HNO}_2]^2 \quad (10)$$

With $A = \exp(37.8) \text{ M}^{-2} \text{ s}^{-1} = 2.6 \times 10^{16} \text{ M}^{-2} \text{ s}^{-1}$ and $E = 65.7 \text{ kJ mol}^{-1}$. At $T = 50^\circ \text{ C}$, this corresponds to a rate constant of $k_9 = A \exp(-E/RT) = 6 \times 10^5 \text{ M}^{-2} \text{ s}^{-1}$. UV photolysis and reduction by Fe^{2+} dominate this process over the $[\text{NO}_2^-]$ range we consider here (Figure 1).

We note that the results of Nguyen et al. (2003) were based on experiments with reactant concentrations $\geq 0.05 \text{ M}$. We assume this rate law to hold at lower concentrations as well; experimental studies are required to confirm this extrapolation. Our overall conclusions do not depend on these kinetics since these reactions are negligible compared to other processes.

2.3 Calculation of $[\text{NO}_x^-]$ in Kinetic Steady-State

We calculate the concentrations of NO_3^- and NO_2^- under the assumption of kinetic steady-state, i.e. that the loss rates of these molecules due to the destruction processes specified in Section 2.2 and summarized in Table 1 equals their supply from the atmosphere (Section 2.1).

To compare loss rates to the supply flux of NO_x^- ($\text{cm}^{-2} \text{ s}^{-1}$), we integrate over the water column, giving us a loss flux ($\text{cm}^{-2} \text{ s}^{-1}$). We consider both ocean and pond environments, corresponding to different families of postulated prebiotic chemistries (e.g., Patel, Percivalle, Ritson, Duffy, and Sutherland (2015) vs. Shibuya et al. (2016)). For the ocean, we adopt a depth of $d_{ocean} = 3.8 \times 10^5 \text{ cm}$, corresponding to the mean depth of the modern ocean (Rumble, 2017). Figure 1 presents the column-integrated destruction rates of oceanic NO_2^- and NO_3^- as functions of $[\text{NO}_2^-]$ and $[\text{NO}_3^-]$, as well as the range of plausible atmospheric supply rates from Wong et al. (2017). The point at which the supply flux equals the destruction flux for a given process corresponds to the steady-state concentration for that process.

Process	Rate Law	Rate Constant
Hydrothermal Vents	$\frac{d[NO_x]}{dt} = k_{vents}[NO_x]$	$k_{vents} = 8 \times 10^{-17} - 1 \times 10^{-14} \text{ s}^{-1}$
NO_2^- UV Photolysis	$\frac{d[NO_2^-]}{dt} = k_{NO_2^-,h\nu}[NO_2^-]$	$k_{NO_2^-,h\nu} = 0.6 - 2.4 \times 10^{-6} \text{ s}^{-1}$
NO_3^- UV Photolysis	$\frac{d[NO_3^-]}{dt} = k_{NO_3^-,h\nu}[NO_3^-]$	$k_{NO_3^-,h\nu} = 1.1 - 4.6 \times 10^{-8} \text{ s}^{-1}$
NO_2^- Reduction by Fe^{2+} to N_2, N_2O	$\frac{d[NO_2^-]}{dt} = k_{NO_2^-,Fe^{2+}}[Fe^{2+}][NO_2^-]$	$k_{NO_2^-,Fe^{2+}} = 2 \times 10^{-6} - 9 \times 10^{-2} \text{ M}^{-1} \text{ s}^{-1}, ([Fe^{2+}] > [NO_2^-]);$ $k_{NO_2^-,Fe^{2+}} = 2 \times 10^{-7} - 9 \times 10^{-3} \text{ M}^{-1} \text{ s}^{-1}, ([Fe^{2+}] < [NO_2^-])$
NO_3^- Reduction by Fe^{2+} to N_2, N_2O	$\frac{d[NO_3^-]}{dt} = k_{NO_3^-,Fe^{2+}}[NO_3^-][Fe^{2+}]$	$k_{NO_3^-,Fe^{2+}} = 0 - 9 \times 10^{-4} \text{ M}^{-1} \text{ s}^{-1}$
NO_2^- Reduction by Fe^{2+} to NH_3	$\frac{d[NH_3]}{dt} = k_7[NO_2^-][Fe^{2+}]^{1.8}$	$k_7 = 4.2 \times 10^{-5} \text{ M}^{-1.8} \text{ s}^{-1}$ (Max.)
Anammox of NO_2^- and NH_3	$\frac{d[N_2]}{dt} = k_9[NH_3][HNO_2]^2$	$k_9 = 6 \times 10^5 \text{ M}^{-2} \text{ s}^{-1}$ ($T = 50^\circ\text{C}$)

Table 1. Summary of NO_x^- loss process kinetics

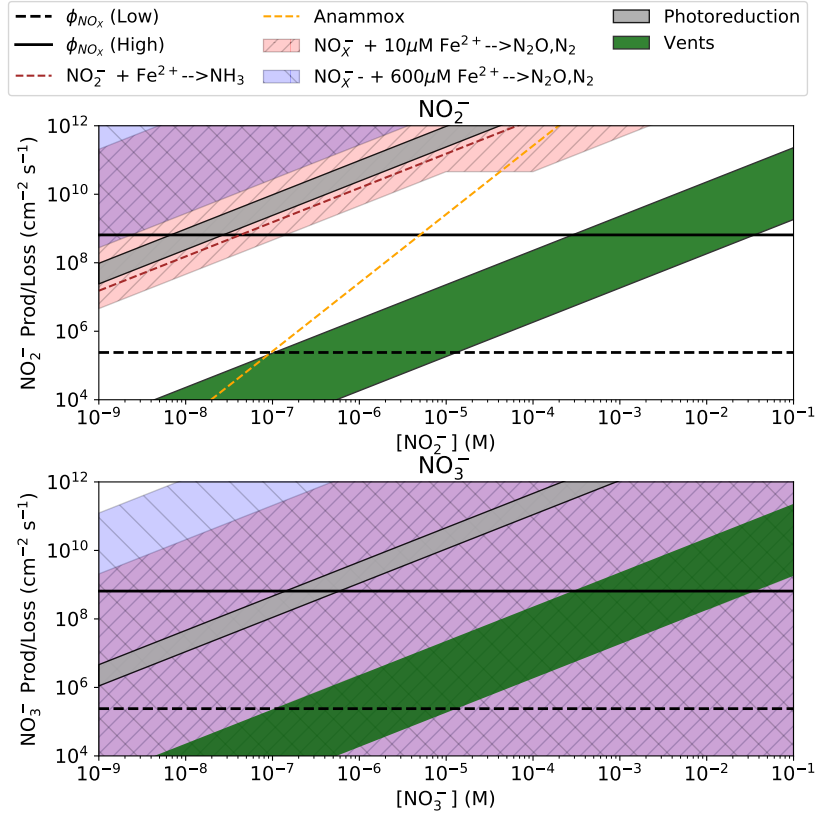


Figure 1. Kinetic loss rates for oceanic NO_2^- (top) and NO_3^- (bottom) for the processes summarized in Table 1, as a function of $[\text{NO}_2^-]$ and $[\text{NO}_3^-]$. Also plotted are the extremal $\phi_{\text{NO}_X^-}$ calculated by Wong et al. (2017). The point at which the supply flux equals the destruction flux for a given process corresponds to the steady-state concentration for that process; the largest destruction flux (leftmost curve at given $\phi_{\text{NO}_X^-}$) dominates the system. Note that NO_3^- reduction by Fe^{2+} cannot be used to set an upper limit on $[\text{NO}_3^-]$, because we consider the possibility that $k_{\text{NO}_3^-, \text{Fe}^{2+}} = 0$.

For pond environments, a broad range of depths is possible. Larger depths correspond to lower $[\text{NO}_X^-]$, since more column is available over which NO_X^- is destroyed (or, equivalently, input NO_X^- flux is distributed over a larger column). To obtain an upper limit on plausible $[\text{NO}_X^-]$, we choose $d_{\text{pond}} = 10$ cm, corresponding approximately to the summer depths of Don Juan Pond in Antarctica, which hosts millimolar abiotic NO_X^- (Marion, 1997; Samarkin et al., 2010; Torii, Yamagata, Ossaka, Murata, et al., 1977). Figure 2 presents the column-integrated destruction rate of pond NO_2^- and NO_3^- as a function of $[\text{NO}_2^-]$ and $[\text{NO}_3^-]$, as well as the range of plausible atmospheric supply rates from Wong et al. (2017). Pond catchment areas can be much larger than their surface areas, meaning that ponds can concentrate atmospherically-delivered NO_X^- if the drainage timescale is short enough that the NO_X^- does not decay en route). The catchment area/surface area ratio is often termed the drainage ratio (DR). A study of catch-

ment areas in southern England indicates means $DR=14$ for lakes and $DR=500$ for ponds (Davies, Biggs, Williams, Lee, & Thompson, 2008). We therefore also present the supply fluxes scaled by a factor of 100, to simulate the potential concentrating effects of high DR.

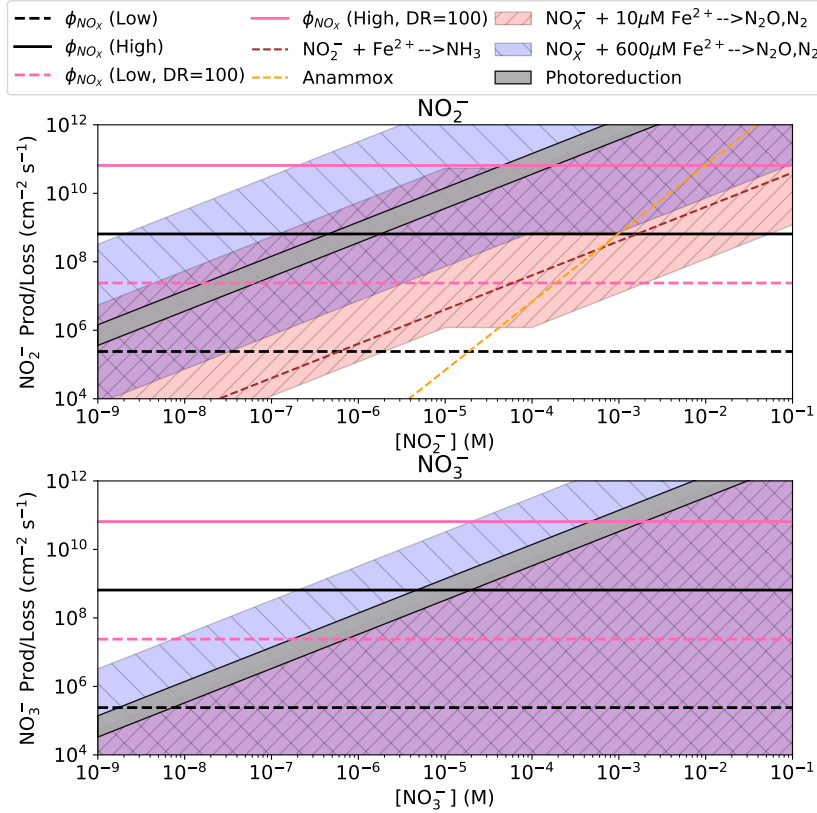


Figure 2. Kinetic loss rates for pond NO_2^- (top) and NO_3^- (bottom) for the processes summarized in Table 1, as a function of $[\text{NO}_2^-]$ and $[\text{NO}_3^-]$. Also plotted are the extremal $\phi_{\text{NO}_x^-}$ calculated by Wong et al. (2017), as well as these $\phi_{\text{NO}_x^-}$ scaled by $100\times$ to simulate a lake/pond with a large DR and fast drainage. The point at which the supply flux equals the destruction flux for a given process corresponds to the steady-state concentration for that process; the largest destruction flux (leftmost curve at given $\phi_{\text{NO}_x^-}$) dominates the system. Note that NO_3^- reduction by Fe^{2+} cannot be used to set an upper limit on $[\text{NO}_3^-]$, because we consider the possibility that $k_{\text{NO}_3^-, \text{Fe}^{2+}} = 0$.

Figures 1 and 2 show that UV photolysis and reduction by Fe^{2+} to nitrogenous gas are the dominant sinks on NO_x^- in natural waters; at a given $[\text{NO}_x^-]$, the loss rates due to these processes are higher than the others, including processing at vents. We calculate $[\text{NO}_2^-]$ and $[\text{NO}_3^-]$ in the ocean as a function of $\phi_{\text{NO}_x^-}$ including UV photolysis and reduction by Fe^{2+} as sinks, and exploring the full range of reaction rate coeffi-

cients identified in Table 1. We assume the NO_x^- is supplied as 80% NO_3^- and 20% NO_2^- , following the experimental work of Summers and Khare (2007); however, our results are not strongly sensitive to this assumption. We repeat this calculation for the case of a shallow pond with high drainage ratio and fast drainage ($d = 10$ cm, $\text{DR} = 100$), corresponding to a highly favorable scenario for NO_x^- accumulation. Hence, this should be considered an approximate upper bound on plausible NO_x^- . From this calculation, the upper bound on oceanic NO_x^- is $< 10\mu\text{M}$, and typically $< 1\mu\text{M}$ across most of parameter space. Ponds with favorable drainage characteristics can accumulate much more NO_x^- (Figure 3).

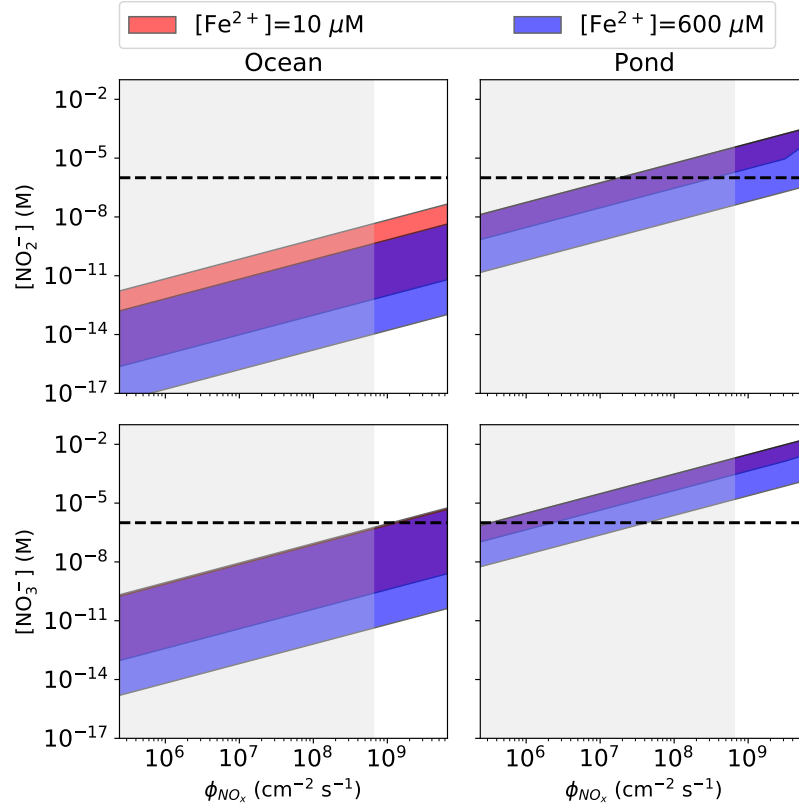


Figure 3. Steady-state concentrations of NO_2^- and NO_3^- as a function of atmospheric supply flux with UV photolysis and reduction by Fe^{2+} to nitrogenous gas as the sinks, in the ocean and in a pond. The pond parameters ($d = 10$ cm, $\text{DR} = 100$) are favorable for NO_x^- accumulation, and hence should be considered an optimistic scenario. The horizontal dashed line demarcates micromolar concentrations, the putative boundary concentration for prebiotic relevance. The grey shaded area corresponds to the range of $\phi_{\text{NO}_x^-}$ calculated by Wong et al. (2017).

2.4 Sensitivity to pH

We have focused on $\text{pH} = 6.5\text{--}8$, motivated by the findings of Halevy and Bachan (2017) and Krissansen-Totton et al. (2018) that the early ocean was circumneutral. However, this finding is a model prediction. Additionally, lakes/ponds can be buffered by local factors to an even wider range of pH; on modern Earth, lake pH ranges from $\text{pH} <$

1 to $\text{pH} > 11$ (Grant & Jones, 2000; Löhr et al., 2005). Here, we consider the sensitivity of our results to our assumption of circumneutral pH.

As measured by OH production, NO_2^- photolysis rates vary by $\leq 2\times$ from $\text{pH} = 4 - 11$, and nitrate photolysis rates by $\leq 3\times$ from $\text{pH} = 2 - 14$, suggesting this process should be insensitive to pH (Daniels, Meyers, & Belardo, 1968; Zafiriou & Bonneau, 1987; Zellner et al., 1990). However, for water with low concentrations of OH scavengers, nitrite photolysis should be reduced, since the OH can react with the photolysis products to reform the nitrite (Zafiriou, 1974; Zafiriou & True, 1979b). Carbonate and bicarbonate are efficient OH scavengers. Consequently, achieving low OH scavenger concentrations requires $\text{pH} < 6$, such that dissolved inorganic carbon is present primarily as CO_2 as opposed to bicarbonate or carbonate at higher pH. At such pH, NO_2^- is unstable. Hence, our choice of photolysis rate constants are valid from $\text{pH} = 4 - 11$.

$k_{\text{NO}_2^-, \text{Fe}^{2+}}$ increases with pH for $\text{pH} = 6 - 8.5$ (Moraghan & Buresh, 1977; Sørensen & Thorling, 1991). For $\text{pH} < 6$, nitrite protonates and self-decomposes (Park & Lee, 1988; Rây et al., 1917). Brown and Drury (1967) report fast reduction of NO_2^- by Fe^{2+} in alkaline solution (Fanning, 2000) (though the experimental temperature is unclear). Thus, $\text{pH} \approx 6$ probably represents a minimum on thermal loss of NO_2^- .

3 Thermochemical Equilibrium

In this section, we examine the stability of NO_3^- and NO_2^- in the anoxic early Earth environment under the assumption of thermal equilibrium. The purpose of this analysis is to test the implicit assumption of previous work that these molecules are stable in prebiotic waters absent processing at vents. Whether or not thermal equilibrium is achieved depends upon kinetic considerations. However, while our understanding of nitrogen kinetics in prebiotic natural waters may be incomplete (since we do not have an anoxic, prebiotic Earth-analog atmosphere-ocean system to study to confirm we have identified all relevant reactions), our equilibrium analysis depends only on known thermodynamic parameters, and hence is robust.

We consider the general speciation of nitrogen in a reducing atmosphere-ocean system as present on early Earth, with H_2 as our reductant ($\text{pH}_2 \geq 1 \times 10^{-3}$ bar on early Earth; Kasting (2014)). We balance the nitrogen-converting redox half reactions with H_2 oxidation and take this to physically represent the amount of "reducing power" in the environment, even though the system could obtain its reducing power from other half reactions, e.g., Fe(II) oxidation. pN_2 on early Earth is known to have been comparable to present-day levels ($0.5 < \text{pN}_2 < 1.1$ bar, Marty et al. (2013)). We consider an initial atmosphere-ocean system with atmospheric $\text{pN}_2 = 1.1$ bar, oceanic $[\text{N}_2]$ in equilibrium with the atmosphere (i.e. saturated in N_2), and no other initial carrier of N. We assume an N_2 -dominated atmosphere and ocean volume equal to modern. Then, the total inventory of nitrogen atoms N_N in the atmosphere/ocean system is:

$$N_N = 2 \times ([\text{N}_2]V_{\text{ocean}} + \left(\frac{\text{pN}_2}{\mu g}\right)(4\pi R_{\text{Earth}}^2)) \quad (11)$$

Here, $V_{\text{ocean}} = 1.4 \times 10^{21}$ L is the volume of the ocean (Pierazzo & Chyba, 1999), $\mu = 28$ g/mol is the mean molecular mass of the N_2 -dominated atmosphere, and $g = 981$ cm s^{-2} is the acceleration due to gravity. From Henry's Law, $[\text{N}_2] = H_{\text{N}_2} \text{pN}_2$, where $H_{\text{N}_2} = 6.4 \times 10^{-4}$ M bar^{-1} (Table 5). Then, $N_N = 4 \times 10^{20}$ mol, comparable to present atmospheric N (Johnson & Goldblatt, 2015).

We allow this N_2 to relax to equilibrium under a range of pH_2 and pH, and calculate the speciation of nitrogen compounds at equilibrium. To do this, we consider the

possible reactions between the nitrogen species by balancing the individual half reactions for interconverting nitrogen species with H_2 oxidation, and calculate cell potentials and logK for each reaction (see also SI, Section S2). We identified the reactions of each species with H_2 with the largest logK; they are tabulated in Table 3. The Gibbs free energies of formation used in this study, ΔG_f° , are compiled in Table 2.

Species	ΔG_f° (kJ/mol)	Reference
NO_3^- (aq)	-111.3	Rumble (2017)
NO_2^- (aq)	-32.2	Rumble (2017)
NH_4^+ (aq)	-79.5	Rumble (2017)
NO (g)	87.6	Rumble (2017)
N_2O (g)	103.7	Rumble (2017)
N_2 (g)	0	Rumble (2017)
N_2 (aq)	18.8	Amend and Shock (2001)
O_2 (g)	0	Rumble (2017)
O_2 (aq)	16.54	Amend and Shock (2001)
H_2 (g)	0	Rumble (2017)
H_2 (aq)	17.72	Amend and Shock (2001)
H_2O	-237.1	Rumble (2017)
H^+	0	Rumble (2017)

Table 2. Gibbs free energies of formation under standard conditions (ΔG_f°) for the species considered in this work.

Number	Reaction	ΔG_{rxn}° (kJ/mol)	E_{cell}° (V)	log K
1	$2NO_3^- + 12H^+ + 10e^- \rightarrow N_2 + 6H_2O$			
	$2NO_3^- + 2H^+ + 5H_2 \rightarrow N_2 + 6H_2O$	-1202	1.25	210.4
2	$2NO_2^- + 8H^+ + 6e^- \rightarrow N_2 + 4H_2O$			
	$2NO_2^- + 2H^+ + 3H_2 \rightarrow N_2 + 4H_2O$	-879.6	1.52	154.0
3	$NO + 6H^+ + 5e^- \rightarrow NH_4^+ + H_2O$			
	$2NO + 2H^+ + 5H_2 \rightarrow 2NH_4^+ + 2H_2O$	-403.3	0.84	141.9
4	$N_2O + 10H^+ + 8e^- \rightarrow 2NH_4^+ + H_2O$			
	$N_2O + 2H^+ + 4H_2 \rightarrow 2NH_4^+ + H_2O$	-499.7	0.65	87.5
5	$N_2 + 8H^+ + 6e^- \rightarrow 2NH_4^+$			
	$N_2 + 2H^+ + 3H_2 \rightarrow 2NH_4^+$	-159.0	0.27	27.8

Table 3. Half reactions and full cell reactions (balanced with H_2 oxidation) with the maximum logK's for the nitrogen species considered in this study. ΔG_{rxn}° , E_{cell}° , and log K were calculated using the standard expressions (SI Section S2)

We use these reactions to set up equations for concentrations at equilibrium using the definition of the equilibrium constant:

$$K_1 = \frac{[N_2]}{[NO_3^-]^2[H^+]^2[H_2]^5} \quad (12)$$

$$K_2 = \frac{[N_2]}{[NO_2^-]^2[H^+]^2[H_2]^3} \quad (13)$$

$$K_3 = \frac{[NH_4^+]^2}{[NO]^2[H^+]^2[H_2]^5} \quad (14)$$

$$K_4 = \frac{[NH_4^+]^2}{[N_2O][H^+]^2[H_2]^4} \quad (15)$$

$$K_5 = \frac{[NH_4^+]^2}{[N_2][H^+]^2[H_2]^3} \quad (16)$$

NO_3^- , NO_2^- , and NH_4^+ undergo further acid/base equilibration, with partitioning governed by the reaction pKa's (Table 4):



$$K_a = \frac{[H^+][A^-]}{[HA]} = 10^{-pK_a} \quad (18)$$

Where A^- is the acid and HA its conjugate base.

Reaction	pKa	Reference
$HNO_3 \leftrightarrow H^+ + NO_3^-$	-1.38	“Lange’s Handbook of Chemistry” (1985)
$HNO_2 \leftrightarrow H^+ + NO_2^-$	3.25	Rumble (2017)
$NH_4^+ \leftrightarrow H^+ + NH_3$	9.25	Rumble (2017)

Table 4. pKa’s for relevant dissociations of acids/bases in the redox network to their corresponding conjugate base/acid.

Aqueous HNO_3 , HNO_2 , NO , N_2O , N_2 , NH_3 exist in equilibrium with their gaseous forms, with partitioning specified by Henry’s Law (Table 5; R. Sander (2015)):

$$[X] = H_X pX \quad (19)$$

Where H_X is the Henry’s Law constant for species X , and pX its partial pressure.

Species	H (M/bar)	Reference
HNO_3	2.6×10^6	Chameides (1984)
HNO_2	5×10^1	Chameides (1984)
NO	1.9×10^{-3}	Schwartz and White (1981)
N_2O	2.4×10^{-2}	R. Sander (2015)
N_2	6.4×10^{-4}	R. Sander (2015)
NH_3	6×10^1	Kavanaugh and Trussell (1980)
O_2 (g)	1.3×10^{-3}	R. Sander (2015)
H_2 (g)	7.8×10^{-4}	R. Sander (2015)

Table 5. Henry’s Law constants (H) under standard conditions and zero salinity for the species considered in this analysis in aqueous solution.

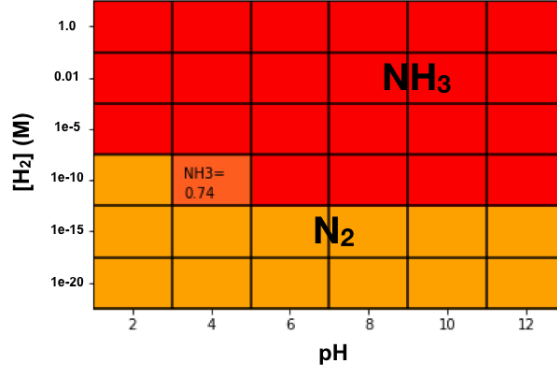


Figure 4. Favored nitrogen species as a function of pH and hydrogen concentration. At high reducing powers ($\geq 10^{-5}$ M H₂), at thermodynamic equilibrium, nitrogen will go to the (-3) oxidation state, i.e. NH₃ or NH₄⁺. Below this reducing power, the favored state of nitrogen is N₂, which partitions mainly to the atmosphere. At pH= 4 and [H₂]= 10⁻¹⁰ M, N₂ and NH₃ coexist. Lower H₂ concentrations are disfavored in conventional models of early Earth and not included in the analysis (Kasting, 1993).

Finally, we have the mass balance constraint that the sum of nitrogen atoms across all species equals the initial nitrogen inventory N_N :

$$N_N = ([NO_3^-] + [NO_2^-] + [NO] + 2[N_2O] + 2[N_2] + [NH_4^+] + [HNO_3] + [HNO_2] + [NH_3])V_{ocean} \quad (20)$$

$$+ \frac{pHNO_3 + pHNO_2 + pNO + 2pN_2O + 2pN_2 + pNH_3}{\mu g} (4\pi R_{Earth}^2) \quad (21)$$

Taken together, this system provides us with 15 equations, 15 unknowns ([NO₃⁻], [NO₂⁻], [NO], [N₂O], [N₂], [NH₄⁺]; [HNO₃], [HNO₂], [NH₃]; pHNO₃, pHNO₂, pNO, pN₂O, pN₂, pNH₃), and 3 prescribed conditions ([H⁺], [H₂], N_N). We solve this system of equations for a range of pH ([H⁺]) and reducing powers ([H₂]) for $N_N = 4 \times 10^{20}$ mol. We compute the fraction of atoms of N stored in each species (Figure 4).

Figure 4 shows the speciation of nitrogen by redox state. The two oxidation states of nitrogen favored under plausible hydrogen concentrations are (-3) and (0), corresponding to NH₃/NH₄⁺ and N₂, respectively. N₂, which is favored at [H₂] ≤ 10⁵ M, will partition mostly into the atmosphere. The distribution of NH₄⁺, NH₃ (aq), and NH₃ (g) depends on the pH of the aqueous solution. The concentration of NO₃⁻ and NO₂⁻ is sub-

picomolar over the scenarios considered here. These findings are insensitive to variations in pK, pKa, and H_X from $T = 2 - 45^\circ \text{C}$, and variations in H_X due to salinity from $[\text{NaCl}] = 0 - 1\text{M}$; see SI Section S3 for details.

Overall, nitrate and nitrite are thermally unstable in the reducing conditions available on early Earth. If allowed to reach equilibrium, under most conditions NO_X^- will relax to a gaseous species like N_2 . This result is consistent with Van Cleemput and Baert (1978), who concluded that NO_2^- in anoxic soils should decay, generally to N_2 . The situation on reducing prebiotic Earth is very different from the situation on oxidizing modern Earth, where in equilibrium NO_X^- is thermodynamically favored (Krissansen-Totton, Bergsman, & Catling, 2016). Our thermochemical analysis confirms our kinetic analysis that previous work has overestimated prebiotic $[\text{NO}_X^-]$, increasing our confidence in this conclusion.

4 Discussion

4.1 $[\text{NO}_X^-]$ in the Prebiotic Oceans

Previous work has concluded that $[\text{NO}_X^-]$ in the prebiotic oceans was high, on the assumption that the dominant sink of NO_X^- in the prebiotic ocean was processing at hydrothermal vents and that it was otherwise stable in the ocean (Laneuville et al., 2018; Wong et al., 2017). However, NO_X^- is thermodynamically unstable in reducing environments. UV photolysis and reduction by Fe^{2+} are much stronger sinks than processing at vents, and restrict NO_X^- to orders of magnitude lower concentrations than previously suggested. Reduction by Fe^{2+} and UV photolysis suppresses NO_X^- to sub-micromolar concentrations across most of the plausible parameter space. $> 1 \mu\text{M}$ NO_X^- requires $\phi_{\text{NO}_X^-} > 1 \times 10^9 \text{cm}^{-2} \text{s}^{-1}$, higher than has been suggested in the literature. Achieving such high $\phi_{\text{NO}_X^-}$ requires some combination of a high lightning flash rate, high pCO_2 , and low pN_2/pCO_2 . The required pCO_2 and pN_2 are not favored by the available geochemical evidence, and we lack a robust prescription for global lightning flash rates, leading us to disfavor this possibility. Consequently, prebiotic oceanic NO_X^- was likely sub-micromolar.

Wong et al. (2017) point out that Fitzsimmons, Boyle, and Jenkins (2014) have detected dissolved iron thousands of kilometers from hydrothermal sources, and suggest that the survival of this iron for such large distances on NO_X^- -rich modern Earth means that Fe^{2+} oxidation, by NO_X^- and other oxidants is inefficient. However, Fitzsimmons et al. (2014) also point out that only 0.02–1% of hydrothermal Fe survives transport over these distances in the dissolved phase, meaning that the vast majority of hydrothermal Fe is oxidized. Moreover, the Fe that does avoid oxidation is thought to do so by forming colloids and/or by complexing with organic ligands (Fitzsimmons et al., 2014; Hawkes, Connelly, Gledhill, & Achterberg, 2013; S. G. Sander & Koschinsky, 2011; Tagliabue, 2014). In other words, hydrothermal Fe appears to survive long-distance transport because it is protected by complexing, mineralization, and colloidation, not because its reactions with oxidants are inefficient. Additionally, mineralized Fe^{2+} is typically a more effective reductant than dissolved Fe^{2+} (Dhakal, 2013; Hansen, Koch, Nancke-Krogh, Borggaard, & Sørensen, 1996; Sørensen & Thorling, 1991). We consequently argue that it is not possible to dismiss reduction by Fe^{2+} as a sink on NO_X^- , especially in light of evidence that Fe^{2+} levels were high on early Earth.

4.2 $[\text{NO}_X^-]$ in Prebiotic Ponds

As in the oceans, reduction by Fe^{2+} and photochemical loss are major sinks of NO_X^- . However, since ponds are much shallower than oceans, the impact of thermal reactions is muted, and UV photolysis is proportionated more important.

$[\text{NO}_x^-]$ could have been above oceanic in shallow ponds ($d \lesssim 3$ m) with large DR and short transit times. Shallow ponds permit higher NO_x^- buildup because NO_x^- destruction processes have a shorter column over which to operate. Large drainage ratios permit ponds to collect NO_x^- rainout from a larger area. Short transit times minimize the probability the NO_x^- will decay en route due to encounters with reductants in the soil. For a pond with $d = 10$ cm, $\text{DR} = 100$, and fast drainage, $[\text{NO}_x^-]$ can build up to micromolar concentrations for $\phi_{\text{NO}_x^-} \geq 4 \times 10^7 \text{ cm}^{-2} \text{ s}^{-1}$, and at lower $\phi_{\text{NO}_x^-}$ if the pond is cold and acidic. For $\phi_{\text{NO}_x^-} = 6.5 \times 10^8 \text{ cm}^{-2} \text{ s}^{-1}$, $[\text{NO}_x^-]$ can build up to near-millimolar concentrations in such a lake.

We consider whether such a pond is plausible. A study of water bodies in southern England indicated that the ratio between the total catchment area and total surface area for lakes and ponds was 14 and 500, respectively, and a study of boreal lakes in Sweden found DR as high as 1000, indicating $\text{DR} = 100$ to be plausible (Davies et al., 2008; Sobek, Algesten, BERGSTRÖM, Jansson, & Tranvik, 2003). Assuming neutral, room-temperature groundwaters with $[\text{Fe}^{2+}] \leq 10^{-4} \text{ M}$, the lifetime of NO_x^- is ≥ 400 days, implying transit times ≤ 400 days are required to ensure negligible decay of NO_x^- during transport. Catchment transit times ≤ 400 days exist, particularly for smaller catchments, but are not universal, indicating that only a subset of ponds will meet this criterion (Brosig, Geyer, Subah, & Sauter, 2008; Broxton, Troch, & Lyon, 2009; McGuire & McDonnell, 2006; Rodhe, Nyberg, & Bishop, 1996). Further, if present, mineralized Fe^{2+} in the ground may more efficiently reduce NO_x^- (Dhakal, 2013). These challenges will be avoided in terrain where rain is immediately lost to the pond as surface runoff; this is especially likely to occur in catchments in bare, rocky terrain (Li et al., 2011). Ponds with high concentrations of NO_x^- do exist on modern Earth, as predicted from our modeling; an example is Don Juan Pond, which is thought to be abiotic and which features $[\text{NO}_x^-] = 6 \text{ mM}$ (Samarkin et al., 2010). In summary, ponds with high $[\text{NO}_x^-]$ should have existed on early Earth, but were probably not typical; hence, pond prebiotic chemistries which require high NO_x^- must specify such a pond as part of their scenario.

4.3 Implications for Prebiotic Chemistry

Oceanic NO_x^- could only have achieved prebiotically relevant levels if atmospheric supply rates were very high. Achieving $[\text{NO}_x^-] \geq 1 \mu\text{M}$ requires $\phi_{\text{NO}_x^-} \geq \times 10^9 \text{ cm}^{-2} \text{ s}^{-1}$, which requires some combination of high flash rates, high pCO_2 , and low pN_2/pCO_2 . These conditions are not at present favored in the literature (Krissansen-Totton et al. (2018); Marty et al. (2013); Wong et al. (2017)). Consequently, oceanic NO_x^- -dependent origin-of-life scenarios (e.g., those that invoke NO_x^- as electron acceptors at deep-sea hydrothermal vents; Ducluzeau et al. (2009); Nitschke and Russell (2013); Shibuya et al. (2016)) must invoke either extreme planetary parameters, or local circumstances which can concentrate $[\text{NO}_x^-]$ levels beyond the oceanic mean.

NO_x^- could have achieved above-oceanic concentrations in favorable pond environments, i.e. ponds with large DR and short catchment transit times. Low temperatures and acidic pH would also favor NO_x^- buildup, especially as NO_3^- . $[\text{NO}_x^-]$ could be even higher at polar latitudes where photolysis rates are suppressed by low UV surface radiances due to larger solar zenith angles (Ranjan & Sasselov, 2017). Such a pond would be able to sustain $[\text{NO}_x^-] \geq 1 \mu\text{M}$ across most of the range of $\phi_{\text{NO}_x^-}$ calculated by Wong et al. (2017). Such ponds are plausible but not typical, and hence must be explicitly invoked when considering NO_x^- -dependent pond prebiotic chemistries. Their non-universality must also be considered when estimating the plausibility of NO_x^- -dependent prebiotic chemistries.

NO_3^- is orders of magnitude more stable than NO_2^- . This suggests that in both lake and oceanic environments, prebiotic NO_x^- should have existed primarily as NO_3^- , as in natural waters on modern Earth and in experimental studies of abiotic nitrogen

fixation (Summers & Khare, 2007). Consequently, NO_3^- -utilizing prebiotic chemistries are more plausible than NO_2^- -dependent prebiotic chemistries, and prebiotic chemists should consider using NO_3^- instead of NO_2^- in their studies.

In this work, we have focused on concentrations of NO_2^- and NO_3^- , under the broad category of NO_X^- . We have ignored more complex derivatives of these compounds. For example, Mariani et al. (2018) point out that under UV irradiation, NO_3^- , Fe, and HCN combine to yield nitroprusside, a compound in which NO_X^- is protected from reduction by Fe^{2+} and which is stable in the dark on a timescale of ≥ 5 months. However, nitroprusside is unstable to irradiation by the visible light which accompanies UV irradiation (Schulz et al., 2010; Van Loenen & Hofs-Kemper, 1979; Vesey & Batistoni, 1977). Measurements of the kinetics of nitroprusside formation and destruction are required to determine the range of plausible steady-state concentrations of nitroprusside in prebiotic natural waters.

We note in passing that the prospects for abiotic NO_X^- buildup may be enhanced on planets orbiting M-dwarfs, due to their much lower surface UV irradiation and consequently much slower NO_X^- photolysis rate (Ranjan, Wordsworth, & Sasselov, 2017). Consequently, NO_X^- -dependent prebiotic chemistries may proceed especially well on such worlds relative to early Earth.

4.4 Validity of Simplifying Assumptions

In this work, we have approximated the activity of ionic species (e.g., NO_3^- , H^+) by their concentrations, neglecting the effects of ion-ion and ion-water interactions on their reactivity. For the species relevant to this work, the activity coefficient $\gamma_C \geq 0.26$ for solutions with ionic strengths $I \leq 1$ (SI Section S1). For context, the ionic strength of the modern oceans is $I = 0.7$, and studies of fluid inclusions in quartz suggests that Archean ocean salinity was \lesssim modern (Marty, Avice, Bekaert, & Broadley, 2018; Rumble, 2017)). Our order-of-magnitude conclusions are insensitive to such variations, motivating this simplifying assumption.

Van Cleemput and Baert (1983) suggest that the kinetics of NO_2^- reduction by Fe^{2+} are second-order with respect to nitrite concentrations at acidic pH. We repeated our analysis assuming second-order dependence on $[\text{NO}_2^-]$; our conclusions were unchanged, indicating our analysis is insensitive to this possibility.

Our photolysis calculations assume photolysis rate constants equal to the modern value. While shortwave surface UV irradiation (200 – 300 nm) on anoxic early Earth was much higher than on modern Earth, surface UV irradiation over the full UV range (200–400 nm) was 20% lower on prebiotic Earth compared to modern Earth, suggesting we may slightly overestimate the photolysis rate (Ranjan & Sasselov, 2017). However, (1) our conclusions are robust to variations in photolysis rate of a few tens of percent, and (2) the magnitude of NO_X^- photolysis is sensitive to the action spectrum of NO_X^- photolysis; if shorter wavelengths are much more effective at photolyzing NO_X^- , then our methods may underestimate photolysis rates (Claire et al., 2012; Cockell, 2000; Ranjan & Sasselov, 2016). Further measurements of the action spectrum of NO_X^- photolysis are required to rule on this possibility.

Our calculations assumes all NO_X^- entering the ocean goes to NO_X^- and neglects reactions of NO_X^- with other reductants which may have been abundant on early Earth, such as H_2 , CH_4 , or Mn^{2+} (Fischer, Hemp, & Valentine, 2016; Tian, Toon, Pavlov, & De Sterck, 2005; Zahnle, Gacesa, & Catling, 2018). Consequently, our estimates should be considered upper bounds on prebiotic $[\text{NO}_X^-]$.

This box-model approach we have taken averages over the entire natural water body under consideration. This approach permits us to place bounds on the mean concentra-

tions of NO_X^- in prebiotic natural waters with minimal assumptions, and is in line with past work (e.g., Laneuville et al. (2018); Wong et al. (2017)). This approach is a good approximation to well-mixed shallow lakes and ponds. However, the oceans are not necessarily well-mixed; $[\text{NO}_X^-]$ may be a function of depth. Resolved, 1D models are required to probe this effect; mean oceanic concentration should be similar, but NO_X^- concentrations should be higher at the surface where it is supplied and lower at depth. In summary, our approach suffices for NO_X^- estimates in ponds, and for estimates of the mean NO_X^- concentration in the ocean, but resolving the heterogeneity of the ocean requires higher-dimensional models.

4.5 Importance of Better Kinetic Constraints

Measurements of NO_X^- kinetics under conditions relevant to the early Earth are scarce. While our calculations are motivated by and consistent with available data, improved measurements of these kinetics can decrease the uncertainty in these calculations and improve the confidence of these results. In particular: (1) the literature contains contradictory reports as to whether uncatalyzed NO_3^- reduction by Fe^{2+} is significant at room temperature (Ottley et al., 1997; Picardal, 2012). Experimental studies are required to resolve the dichotomy between these studies; if this process is indeed significant, as Ottley et al. (1997) report, then oceanic NO_3^- concentrations would be suppressed to concentrations lower than we model here. (2) The activation energy for reduction of NO_2^- by Fe^{2+} is not known; knowledge of this quantity would enable tighter constraints on $k_{\text{NO}_2^-, \text{Fe}^{2+}} > 0$. (3) The rate constants for Fe^{2+} reduction used in this work are generally derived from measurements made at larger $[\text{Fe}^{2+}]$ than thought to have been available on early Earth. Determination of these rate constants at prebiotically plausible $[\text{Fe}^{2+}]$ (10–600 μM) under early Earth conditions (e.g., anoxia) could confirm the applicability of these rate constants at lower $[\text{Fe}^{2+}]$. The extension of studies like Stanton et al. (2018) for NO kinematics to NO_X^- kinematics could improve the precision and potentially accuracy of this work. (4) Measuring the rate constant of NO_X^- photolysis in simulated prebiotic natural waters, under irradiation by a source simulating the prebiotic UV environment in both magnitude and spectral shape, could directly verify our extrapolation from modern photolysis rates, and in particular could confirm whether the shorter-wavelength UV radiation available on early Earth would affect overall reaction rates.

5 Conclusions

Constraining the abundance of trace chemical species on early Earth is relevant to understanding the plausibility and guiding the development of proposed prebiotic chemistries. In this work, we have used box-model kinetic calculations to constrain the plausible range of NO_2^- and NO_3^- concentrations in oceans and ponds on prebiotic Earth.

Prebiotic oceanic NO_X^- was likely much lower than calculated in previous work (Laneuville et al., 2018; Wong et al., 2017) due to UV photolysis and reactions with Fe^{2+} . Oceanic NO_X^- could only have built up to $\geq 1 \mu\text{M}$ in an extremal realm of parameter space, in particular if the NO_X^- supply flux was much higher than currently favored in the literature. Consequently, origins-of-life scenarios which require elevated NO_X^- in the ocean must invoke either an extremal planetary conditions, or specialized local conditions which concentrate NO_X^- above the oceanic mean. NO_X^- was not an inevitable part of the prebiotic milieu, and the prebiotic plausibility of oceanic origin-of-life scenarios can be improved by utilizing alternative feedstocks, e.g. an alternative electron donor for protometabolism (Ducluzeau et al., 2009).

Prebiotic NO_X^- could have build above oceanic levels in shallow ponds with large, fast-draining catchment areas. Such environments should have been extant but likely uncommon. In these environments, NO_X^- could have built up to prebiotically relevant levels ($\geq 1\mu\text{M}$) over a much broader range of planetary parameters than in the ocean, and

in particular over most (but not all) of the proposed range of NO_X^- supply flux. Consequently, NO_X^- -dependent prebiotic chemistries which can function in shallow ponds (e.g., Mariani et al. (2018)) are prebiotically plausible, with the caveat that they impose requirements on the environment. Near-millimolar NO_X^- concentrations are possible if the NO_X^- supply flux was at the upper end of what has been proposed in the literature ($\phi_{\text{NO}_X^-} \geq 6.5 \times 10^8 \text{cm}^{-2}\text{s}^{-1}$), and if the pond were cool and mildly acidic. This finding is in line with past work which suggests shallow lakes/ponds to be especially compelling venues for origin-of-life chemistry (Deamer & Damer, 2017; Mulkidjanian, Bychkov, Dibrova, Galperin, & Koonin, 2012; Patel et al., 2015; Ranjan et al., 2018). We emphasize that our estimates are upper bounds; if a significant fraction of input NO_X^- failed to go to NO_X^- , or reactions with other reductants present on early Earth were significant compared to the processes considered here, $[\text{NO}_X^-]$ would have been proportionately lower.

For both oceanic and pond environments, NO_X^- -dependent prebiotic chemistries that can function at lower $[\text{NO}_X^-]$ are more prebiotically plausible. Similarly, prebiotic chemistries that utilize NO_3^- are more plausible than those which utilize NO_2^- , since most NO_X^- should be present as NO_3^- due to its greater stability.

Our analysis could be most improved by better characterization of NO_X^- reaction kinetics under prebiotically-relevant conditions, especially its reduction by Fe^{2+} and Mn^{2+} and its reduction by UV in prebiotic natural waters (e.g., the extension of studies like Stanton et al. (2018) to NO_X^-). Studies with higher-dimensional models could also help determine if there exist areas in the ocean which should have concentrated NO_X^- above the oceanic mean, perhaps to prebiotically-relevant levels.

Acknowledgments

We thank Jonathan Toner for help with PHREEQC and insights regarding activity coefficients and diffusion. We thank Joshua Krissansen-Totton for a tutorial on his code, and discussions about thermal equilibrium. We thank Noah Planavsky, Clark Johnson, Scott Wankel, Taylor Perron, Sam Goldberg, William Bains, Craig Walton, and Sara Seager for helpful discussions. We thank Peter Gao, Matthie Laneuville, and Oliver Zafriou for answers to questions. We thank the MIT Libraries for heroic efforts in uncovering very old, very obscure papers. We thank our referees and editor for feedback which substantively improved this paper. Z. R. T. and D. D. S thank the Harvard Origins of Life Initiative. This research has made use of NASA’s Astrophysics Data System. This work was supported by grants from the Simons Foundation (SCOL grant # 495062 to S.R.; grant # 290360 to D.D.S.), and support from an MIT startup (A.R.B.). P.B.R. thanks the Simons Foundation and Kavli Foundation for funding.

The software used to carry out our calculations is available for validation and extension at <https://github.com/sukritranjan/nox.git>.

The authors declare no conflicts of interest with respect to the results of this paper.

References

- Airapetian, V. S., Glocer, A., Gronoff, G., Hébrard, E., & Danchi, W. (2016, June). Prebiotic chemistry and atmospheric warming of early Earth by an active young Sun. *Nature Geoscience*, *9*, 452-455. doi: 10.1038/ngeo2719
- Amend, J. P., & Shock, E. L. (2001). Energetics of overall metabolic reactions of thermophilic and hyperthermophilic archaea and bacteria. *FEMS microbiology reviews*, *25*(2), 175–243.
- Ardaseva, A., Rimmer, P. B., Waldmann, I., Rocchetto, M., Yurchenko, S. N., Helling, C., & Tennyson, J. (2017, September). Lightning chemistry on

- Earth-like exoplanets. *Monthly Notices of the Royal Astronomical Society*, 470, 187-196. doi: 10.1093/mnras/stx1012
- Babbin, A. R., Keil, R. G., Devol, A. H., & Ward, B. B. (2014). Organic matter stoichiometry, flux, and oxygen control nitrogen loss in the ocean. *Science*, 344(6182), 406-408.
- Bada, J. L., Bigham, C., & Miller, S. L. (1994, February). Impact Melting of Frozen Oceans on the Early Earth: Implications for the Origin of Life. *Proceedings of the National Academy of Science*, 91, 1248-1250. doi: 10.1073/pnas.91.4.1248
- Brandes, J. A., Boctor, N. Z., Cody, G. D., Cooper, B. A., Hazen, R. M., & Yoder Jr, H. S. (1998). Abiotic nitrogen reduction on the early earth. *Nature*, 395(6700), 365.
- Brosig, K., Geyer, T., Subah, A., & Sauter, M. (2008). Travel time based approach for the assessment of vulnerability of karst groundwater: the transit time method. *Environmental geology*, 54(5), 905-911.
- Brown, L., & Drury, J. (1967). Nitrogen-isotope effects in the reduction of nitrate, nitrite, and hydroxylamine to ammonia. i. in sodium hydroxide solution with fe (ii). *The Journal of Chemical Physics*, 46(7), 2833-2837.
- Broxton, P. D., Troch, P. A., & Lyon, S. W. (2009). On the role of aspect to quantify water transit times in small mountainous catchments. *Water Resources Research*, 45(8).
- Buchwald, C., Grabb, K., Hansel, C. M., & Wankel, S. D. (2016). Constraining the role of iron in environmental nitrogen transformations: dual stable isotope systematics of abiotic no₂-reduction by fe (ii) and its production of n₂o. *Geochimica et Cosmochimica Acta*, 186, 1-12.
- Canfield, D. E., Glazer, A. N., & Falkowski, P. G. (2010, October). The Evolution and Future of Earth's Nitrogen Cycle. *Science*, 330, 192. doi: 10.1126/science.1186120
- Carpenter, L. J., & Nightingale, P. D. (2015). Chemistry and release of gases from the surface ocean. *Chemical reviews*, 115(10), 4015-4034.
- Chameides, W. L. (1984). The photochemistry of a remote marine stratiform cloud. *Journal of Geophysical Research: Atmospheres*, 89(D3), 4739-4755.
- Claire, M. W., Sheets, J., Cohen, M., Ribas, I., Meadows, V. S., & Catling, D. C. (2012, September). The Evolution of Solar Flux from 0.1 nm to 160 μ m: Quantitative Estimates for Planetary Studies. *Astrophysical Journal*, 757, 95. doi: 10.1088/0004-637X/757/1/95
- Cloud, P. (1973). Paleocological significance of the banded iron-formation. *Economic Geology*, 68(7), 1135-1143.
- Cockell, C. S. (2000, February). The ultraviolet history of the terrestrial planets - implications for biological evolution. *Planetary and Space Science*, 48, 203-214. doi: 10.1016/S0032-0633(99)00087-2
- Corliss, J. B., Baross, J., & Hoffman, S. (1981). An hypothesis concerning the relationships between submarine hot springs and the origin of life on earth. *Oceanologica Acta, Special issue*.
- Cronin, T. W. (2014, August). On the Choice of Average Solar Zenith Angle. *Journal of Atmospheric Sciences*, 71, 2994-3003. doi: 10.1175/JAS-D-13-0392.1
- Daniels, M., Meyers, R., & Belardo, E. (1968). Photochemistry of the aqueous nitrate system. i. excitation in the 300-m. mu. band. *The Journal of Physical Chemistry*, 72(2), 389-399.
- Davies, B., Biggs, J., Williams, P., Lee, J., & Thompson, S. (2008). A comparison of the catchment sizes of rivers, streams, ponds, ditches and lakes: implications for protecting aquatic biodiversity in an agricultural landscape. *Hydrobiologia*, 597(1), 7-17.
- Deamer, D., & Damer, B. (2017). Can life begin on enceladus? a perspective from hydrothermal chemistry. *Astrobiology*.
- Dhakal, P. (2013). *Abiotic nitrate and nitrite reactivity with iron oxide minerals*

- (Unpublished doctoral dissertation). University of Kentucky.
- Ducluzeau, A.-L., Van Lis, R., Duval, S., Schoepp-Cothenet, B., Russell, M. J., & Nitschke, W. (2009). Was nitric oxide the first deep electron sink? *Trends in biochemical sciences*, *34*(1), 9–15.
- Fani, R., Gallo, R., & Lio, P. (2000). Molecular evolution of nitrogen fixation: the evolutionary history of the nifD, nifK, nifE, and nifN genes. *Journal of Molecular Evolution*, *51*(1), 1–11.
- Fanning, J. C. (2000). The chemical reduction of nitrate in aqueous solution. *Coordination Chemistry Reviews*, *199*(1), 159–179.
- Farquhar, J., Bao, H., & Thiemens, M. (2000, August). Atmospheric Influence of Earth's Earliest Sulfur Cycle. *Science*, *289*, 756–759. doi: 10.1126/science.289.5480.756
- Farquhar, J., Savarino, J., Airieau, S., & Thiemens, M. H. (2001, December). Observation of wavelength-sensitive mass-independent sulfur isotope effects during SO₂ photolysis: Implications for the early atmosphere. *Journal of Geophysics Research*, *106*, 32829–32840. doi: 10.1029/2000JE001437
- Fischer, W. W., Hemp, J., & Valentine, J. S. (2016). How did life survive earth's great oxygenation? *Current opinion in chemical biology*, *31*, 166–178.
- Fitzsimmons, J. N., Boyle, E. A., & Jenkins, W. J. (2014, November). Distal transport of dissolved hydrothermal iron in the deep South Pacific Ocean. *Proceedings of the National Academy of Science*, *111*, 16654–16661. doi: 10.1073/pnas.1418778111
- Grabb, K. C., Buchwald, C., Hansel, C. M., & Wankel, S. D. (2017). A dual nitrite isotopic investigation of chemodenitrification by mineral-associated Fe(II) and its production of nitrous oxide. *Geochimica et Cosmochimica Acta*, *196*, 388–402.
- Grant, W., & Jones, B. (2000). Alkaline environments. In J. Lederberg (Ed.), *Encyclopaedia of microbiology* (Vol. 1, pp. 126–133). Academic Press, London and New York.
- Halevy, I., & Bachan, A. (2017, March). The geologic history of seawater pH. *Science*, *355*, 1069–1071. doi: 10.1126/science.aal4151
- Hansen, H. C. B., Koch, C. B., Nancke-Krogh, H., Borggaard, O. K., & Sørensen, J. (1996). Abiotic nitrate reduction to ammonium: key role of green rust. *Environmental Science & Technology*, *30*(6), 2053–2056.
- Hawkes, J. A., Connelly, D. P., Gledhill, M., & Achterberg, E. P. (2013, August). The stabilisation and transportation of dissolved iron from high temperature hydrothermal vent systems. *Earth and Planetary Science Letters*, *375*, 280–290. doi: 10.1016/j.epsl.2013.05.047
- Johnson, B., & Goldblatt, C. (2015). The nitrogen budget of earth. *Earth-Science Reviews*, *148*, 150–173.
- Johnson, B. W., & Goldblatt, C. (2017, September). A secular increase in continental crust nitrogen during the Precambrian. *ArXiv e-prints*.
- Jones, L. C., Peters, B., Lezama Pacheco, J. S., Casciotti, K. L., & Fendorf, S. (2015). Stable isotopes and iron oxide mineral products as markers of chemodenitrification. *Environmental science & technology*, *49*(6), 3444–3452.
- Kasting, J. F. (1982, April). Stability of ammonia in the primitive terrestrial atmosphere. *Journal of Geophysics Research*, *87*, 3091–3098. doi: 10.1029/JC087iC04p03091
- Kasting, J. F. (1993, February). Earth's early atmosphere. *Science*, *259*, 920–926. doi: 10.1126/science.259.5097.920
- Kasting, J. F. (2014). Atmospheric composition of hadean–early archean earth: The importance of CO. *Geological Society of America Special Papers*, *504*, 19–28.
- Kasting, J. F., & Walker, J. C. G. (1981, February). Limits on oxygen concentration in the prebiological atmosphere and the rate of abiotic fixation of nitrogen. *Journal of Geophysical Research*, *86*, 1147–1158. doi:

- 10.1029/JC086iC02p01147
- Kavanaugh, M. C., & Trussell, R. R. (1980). Design of aeration towers to strip volatile contaminants from drinking water. *Journal-American Water Works Association*, *72*(12), 684–692.
- Klein, C. (2005). Some precambrian banded iron-formations (bifs) from around the world: Their age, geologic setting, mineralogy, metamorphism, geochemistry, and origins. *American Mineralogist*, *90*(10), 1473–1499.
- Konhauser, K. O., Planavsky, N. J., Hardisty, D. S., Robbins, L. J., Warchola, T. J., Haugaard, R., ... others (2017). Iron formations: A global record of neoproterozoic to palaeoproterozoic environmental history. *Earth-Science Reviews*, *172*, 140–177.
- Krissansen-Totton, J., Bergsman, D. S., & Catling, D. C. (2016, January). On Detecting Biospheres from Chemical Thermodynamic Disequilibrium in Planetary Atmospheres. *Astrobiology*, *16*, 39–67. doi: 10.1089/ast.2015.1327
- Krissansen-Totton, J., Olson, S., & Catling, D. C. (2018, January). Disequilibrium biosignatures over Earth history and implications for detecting exoplanet life. *Science Advances*, *4*, eaao5747. doi: 10.1126/sciadv.aao5747
- Krissansen-Totton, J., Arney, G. N., & Catling, D. C. (2018). Constraining the climate and ocean pH of the early earth with a geological carbon cycle model. *Proceedings of the National Academy of Sciences*, 201721296.
- Laneville, M., Kameya, M., & Cleaves, H. J. (2018). Earth without life: A systems model of a global abiotic nitrogen cycle. *Astrobiology*.
- Lange's handbook of chemistry. (1985). In J. A. Dean (Ed.), (13th ed., p. 5-16). New York, NY: McGraw-Hill Book Co.
- Li, W., Czaja, A. D., Van Kranendonk, M. J., Beard, B. L., Roden, E. E., & Johnson, C. M. (2013, November). An anoxic, Fe(II)-rich, U-poor ocean 3.46 billion years ago. *Geochimica Cosmochimica Acta*, *120*, 65–79. doi: 10.1016/j.gca.2013.06.033
- Li, X.-Y., Contreras, S., Solé-Benet, A., Cantón, Y., Domingo, F., Lázaro, R., ... Puigdefábregas, J. (2011). Controls of infiltration–runoff processes in mediterranean karst rangelands in se Spain. *Catena*, *86*(2), 98–109.
- Löhr, A., Bogaard, T., Heikens, A., Hendriks, M., Sumarti, S., Bergen, M. v., ... Widianarko, B. (2005). Natural pollution caused by the extremely acid crater lake Kawah Ijen, East Java, Indonesia (7 pp). *Environmental Science and Pollution Research*, *12*(2), 89–95.
- Lomas, M. W., & Lipschultz, F. (2006). Forming the primary nitrite maximum: Nitrifiers or phytoplankton? *Limnology and Oceanography*, *51*(5), 2453–2467.
- Mack, J., & Bolton, J. R. (1999). Photochemistry of nitrite and nitrate in aqueous solution: a review. *Journal of Photochemistry and Photobiology A: Chemistry*, *128*(1-3), 1–13.
- Mancinelli, R. L., & McKay, C. P. (1988, December). The evolution of nitrogen cycling. *Origins of Life*, *18*, 311–325. doi: 10.1007/BF01808213
- Mariani, A., Russell, D. A., Javelle, T., & Sutherland, J. D. (2018). A light-releasable potentially prebiotic nucleotide activating agent. *Journal of the American Chemical Society*.
- Marion, G. (1997). A theoretical evaluation of mineral stability in Don Juan Pond, Wright Valley, Victoria Land. *Antarctic Science*, *9*(1), 92–99.
- Martin, W., Baross, J., Kelley, D., & Russell, M. J. (2008). Hydrothermal vents and the origin of life. *Nature Reviews Microbiology*, *6*(11), 805–814.
- Marty, B., Avice, G., Bekaert, D. V., & Broadley, M. W. (2018). Salinity of the archaean oceans from analysis of fluid inclusions in quartz. *Comptes Rendus Geoscience*, *350*(4), 154–163.
- Marty, B., Zimmermann, L., Pujol, M., Burgess, R., & Philippot, P. (2013, October). Nitrogen Isotopic Composition and Density of the Archaean Atmosphere. *Science*, *342*, 101–104. doi: 10.1126/science.1240971

- McGuire, K. J., & McDonnell, J. J. (2006). A review and evaluation of catchment transit time modeling. *Journal of Hydrology*, *330*(3-4), 543–563.
- Minero, C., Chiron, S., Falletti, G., Maurino, V., Pelizzetti, E., Ajassa, R., . . . Vione, D. (2007). Photochemical processes involving nitrite in surface water samples. *Aquatic Sciences*, *69*(1), 71–85.
- Mojzsis, S. J., Harrison, T. M., & Pidgeon, R. T. (2001, January). Oxygen-isotope evidence from ancient zircons for liquid water at the Earth’s surface 4,300Myr ago. *Nature*, *409*, 178-181.
- Moraghan, J., & Buresh, R. (1977). Chemical reduction of nitrite and nitrous oxide by ferrous iron 1. *Soil Science Society of America Journal*, *41*(1), 47–50.
- Mulkidjanian, A. Y., Bychkov, A. Y., Dibrova, D. V., Galperin, M. Y., & Koonin, E. V. (2012, April). PNAS Plus: Origin of first cells at terrestrial, anoxic geothermal fields. *Proceedings of the National Academy of Science*, *109*, E821-E830. doi: 10.1073/pnas.1117774109
- Mvondo, D. N., Navarro-González, R., McKay, C. P., Coll, P., & Raulin, F. (2001). Production of nitrogen oxides by lightning and coroneae discharges in simulated early earth, venus and mars environments. *Advances in Space Research*, *27*(2), 217–223.
- Navarro-González, R., Molina, M. J., & Molina, L. T. (1998). Nitrogen fixation by volcanic lightning in the early earth. *Geophysical Research Letters*, *25*(16), 3123–3126.
- Nguyen, D. A., Iwaniw, M. A., & Fogler, H. S. (2003). Kinetics and mechanism of the reaction between ammonium and nitrite ions: experimental and theoretical studies. *Chemical engineering science*, *58*(19), 4351–4362.
- Nitschke, W., & Russell, M. J. (2013). Beating the acetyl coenzyme a-pathway to the origin of life. *Phil. Trans. R. Soc. B*, *368*(1622), 20120258.
- Olsen, A., Key, R. M., van Heuven, S., Lauvset, S. K., Velo, A., Lin, X., . . . others (2016). The global ocean data analysis project version 2 (glodapv2)—an internally consistent data product for the world ocean. *Earth System Science Data (Online)*, *8*(2).
- Ottley, C., Davison, W., & Edmunds, W. (1997). Chemical catalysis of nitrate reduction by iron (ii). *Geochimica et Cosmochimica acta*, *61*(9), 1819–1828.
- Park, J. Y., & Lee, Y. N. (1988). Solubility and decomposition kinetics of nitrous acid in aqueous solution. *The Journal of Physical Chemistry*, *92*(22), 6294–6302.
- Patel, B. H., Percivalle, C., Ritson, D. J., Duffy, C. D., & Sutherland, J. D. (2015, April). Common origins of RNA, protein and lipid precursors in a cyanosulfidic protometabolism. *Nature Chemistry*, *7*, 301-307. doi: 10.1038/nchem.2202
- Petersen, H. S. (1979). Reduction of nitrate by iron (ii). *Acta chemica Scandinavica. Series A: Physical and inorganic chemistry*.
- Picardal, F. (2012). Abiotic and microbial interactions during anaerobic transformations of fe (ii) and nox. *Frontiers in microbiology*, *3*, 112.
- Pierazzo, E., & Chyba, C. F. (1999, November). Amino acid survival in large cometary impacts. *Meteoritics and Planetary Science*, *34*, 909-918. doi: 10.1111/j.1945-5100.1999.tb01409.x
- Postma, D. (1990). Kinetics of nitrate reduction by detrital fe (ii)-silicates. *Geochimica et Cosmochimica Acta*, *54*(3), 903–908.
- Ranjan, S., & Sasselov, D. D. (2016, January). Influence of the UV Environment on the Synthesis of Prebiotic Molecules. *Astrobiology*, *16*, 68-88. doi: 10.1089/ast.2015.1359
- Ranjan, S., & Sasselov, D. D. (2017, March). Constraints on the Early Terrestrial Surface UV Environment Relevant to Prebiotic Chemistry. *Astrobiology*, *17*, 169-204. doi: 10.1089/ast.2016.1519
- Ranjan, S., Todd, Z. R., Sutherland, J. D., & Sasselov, D. D. (2018). Sulfidic anion concentrations on early earth for surficial origins-of-life chemistry. *Astrobi-*

ology.

- Ranjan, S., Wordsworth, R., & Sasselov, D. D. (2017). The surface uv environment on planets orbiting m??dwarfs: Implications for prebiotic chemistry and the need for experimental follow-up. *The Astrophysical Journal*, *843*(2), 110. Retrieved from <http://stacks.iop.org/0004-637X/843/i=2/a=110>
- Rây, P. C., Dey, M. L., & Ghosh, J. C. (1917). Xxxvi.?velocity of decomposition and the dissociation constant of nitrous acid. *Journal of the Chemical Society, Transactions*, *111*, 413–417.
- Revsbech, N. P., Larsen, L. H., Gundersen, J., Dalsgaard, T., Ulloa, O., & Thamdrup, B. (2009). Determination of ultra-low oxygen concentrations in oxygen minimum zones by the stox sensor. *Limnology and Oceanography: Methods*, *7*(5), 371–381.
- Rodhe, A., Nyberg, L., & Bishop, K. (1996). Transit times for water in a small till catchment from a step shift in the oxygen 18 content of the water input. *Water Resources Research*, *32*(12), 3497–3511.
- Ruiz-Mirazo, K., Briones, C., & de la Escosura, A. (2014). Prebiotic systems chemistry: new perspectives for the origins of life. *Chem. Rev*, *114*(1), 285–366.
- Rumble, J. R. (Ed.). (2017). *Crc handbook of chemistry and physics* (98th ed.). Boca Raton, FL: CRC Press.
- Samarkin, V. A., Madigan, M. T., Bowles, M. W., Casciotti, K. L., Priscu, J. C., McKay, C. P., & Joye, S. B. (2010, May). Abiotic nitrous oxide emission from the hypersaline Don Juan Pond in Antarctica. *Nature Geoscience*, *3*, 341-344. doi: 10.1038/ngeo847
- Sander, R. (2015, April). Compilation of Henry’s law constants (version 4.0) for water as solvent. *Atmospheric Chemistry & Physics*, *15*, 4399-4981. doi: 10.5194/acp-15-4399-2015
- Sander, S. G., & Koschinsky, A. (2011, March). Metal flux from hydrothermal vents increased by organic complexation. *Nature Geoscience*, *4*, 145-150. doi: 10.1038/ngeo1088
- Santoro, A. E., Sakamoto, C. M., Smith, J. M., Plant, J. N., Gehman, A. L., Worden, A. Z., ... Casciotti, K. L. (2013). Measurements of nitrite production in and around the primary nitrite maximum in the central california current. *Biogeosciences*, *10*(11), 7395–7410. Retrieved from <https://www.biogeosciences.net/10/7395/2013/> doi: 10.5194/bg-10-7395-2013
- Schulz, L. T., Elder, E. J., Jones, K. J., Vijayan, A., Johnson, B. D., Medow, J. E., & Vermeulen, L. (2010). Stability of sodium nitroprusside and sodium thiosulfate 1: 10 intravenous admixture. *Hospital pharmacy*, *45*(10), 779–784.
- Schwartz, S., & White, W. (1981). Solubility equilibria of the nitrogen oxides and oxyacids in dilute aqueous solution. In *Advances in environmental science and engineering. vol. 4*.
- Shibuya, T., Russell, M. J., & Takai, K. (2016). Free energy distribution and hydrothermal mineral precipitation in hadean submarine alkaline vent systems: Importance of iron redox reactions under anoxic conditions. *Geochimica et Cosmochimica Acta*, *175*, 1–19.
- Sobek, S., Algesten, G., BERGSTRÖM, A.-K., Jansson, M., & Tranvik, L. J. (2003). The catchment and climate regulation of pco2 in boreal lakes. *Global Change Biology*, *9*(4), 630–641.
- Sørensen, J., & Thorling, L. (1991). Stimulation by lepidocrocite (7-feooh) of fe (ii)-dependent nitrite reduction. *Geochimica et Cosmochimica Acta*, *55*(5), 1289–1294.
- Spokes, L. J., & Liss, P. S. (1996). Photochemically induced redox reactions in seawater, ii. nitrogen and iodine. *Marine chemistry*, *54*(1-2), 1–10.
- Stanton, C. L., Reinhard, C. T., Kasting, J. F., Ostrom, N. E., Haslun, J. A., Lyons, T. W., & Glass, J. B. (2018). Nitrous oxide from chemodenitrification: A possible missing link in the proterozoic greenhouse and the evolution of aerobic

- respiration. *Geobiology*, 16(6), 597–609.
- Stüeken, E. E., Buick, R., Guy, B. M., & Koehler, M. C. (2015). Isotopic evidence for biological nitrogen fixation by molybdenum-nitrogenase from 3.2 gyr. *Nature*, 520(7549), 666.
- Summers, D. P. (2005). Ammonia formation by the reduction of nitrite/nitrate by fcs: ammonia formation under acidic conditions. *Origins of Life and Evolution of Biospheres*, 35(4), 299–312.
- Summers, D. P., & Chang, S. (1993, October). Prebiotic ammonia from reduction of nitrite by iron (II) on the early Earth. *Nature*, 365, 630-633. doi: 10.1038/365630a0
- Summers, D. P., & Khare, B. (2007, May). Nitrogen Fixation on Early Mars and Other Terrestrial Planets: Experimental Demonstration of Abiotic Fixation Reactions to Nitrite and Nitrate. *Astrobiology*, 7, 333-341. doi: 10.1089/ast.2006.0032
- Tagliabue, A. (2014, November). More to hydrothermal iron input than meets the eye. *Proceedings of the National Academy of Science*, 111, 16641-16642. doi: 10.1073/pnas.1419829111
- Tian, F., Toon, O. B., Pavlov, A. A., & De Sterck, H. (2005, May). A Hydrogen-Rich Early Earth Atmosphere. *Science*, 308, 1014-1017. doi: 10.1126/science.1106983
- Todd, Z. R., Fahrenbach, A. C., Magnani, C. J., Ranjan, S., Björkbom, A., Szostak, J. W., & Sasselov, D. D. (2018). Solvated-electron production using cyanocuprates is compatible with the uv-environment on a hadean–archaeon earth. *Chemical Communications*.
- Torii, T., Yamagata, N., Ossaka, J., Murata, S., et al. (1977). Salt balance in the don juan basin.
- Tosca, N. J., Guggenheim, S., & Pufahl, P. K. (2016, March). An authigenic origin for Precambrian greenalite: Implications for iron formation and the chemistry of ancient seawater. *Geological Society of America Bulletin*, 128, 511-530. doi: 10.1130/B31339.1
- Treinin, A., & Hayon, E. (1970). Absorption spectra and reaction kinetics of no₂, n₂o₃, and n₂o₄ in aqueous solution. *Journal of the American Chemical Society*, 92(20), 5821–5828.
- Urey, H. C. (1952, April). On the Early Chemical History of the Earth and the Origin of Life. *Proceedings of the National Academy of Science*, 38, 351-363. doi: 10.1073/pnas.38.4.351
- Van Cleemput, O., & Baert, L. (1978). Calculations of the nitrite decomposition reactions in soils. In *3. international symposium on environmental biogeochemistry. wolfenbuettel (germany, fr). 1978*.
- Van Cleemput, O., & Baert, L. (1983). Nitrite stability influenced by iron compounds. *Soil Biology and Biochemistry*, 15(2), 137–140.
- Van Loenen, A., & Hofs-Kemper, W. (1979). Stability and degradation of sodium nitroprusside. *Pharmaceutisch weekblad*, 1(1), 424–436.
- Vesey, C., & Batistoni, G. (1977). The determination and stability of sodium nitroprusside in aqueous solutions (determination and stability of snp). *Journal of Clinical Pharmacy and Therapeutics*, 2(2), 105–117.
- Walker, J. C., & Brimblecombe, P. (1985). Iron and sulfur in the pre-biologic ocean. *Precambrian Research*, 28(3-4), 205–222.
- Wong, M. L., Charnay, B. D., Gao, P., Yung, Y. L., & Russell, M. J. (2017, October). Nitrogen Oxides in Early Earth’s Atmosphere as Electron Acceptors for Life’s Emergence. *Astrobiology*, 17, 975-983. doi: 10.1089/ast.2016.1473
- Xu, J., Ritson, D. J., Ranjan, S., Todd, Z. R., Sasselov, D. D., & Sutherland, J. D. (2018). Photochemical reductive homologation of hydrogen cyanide using sulfite and ferrocyanide. *Chemical Communications*.

- Zafriou, O. C. (1974). Sources and reactions of $^{\bullet}\text{OH}$ and daughter radicals in seawater. *Journal of Geophysical Research*, 79(30), 4491–4497.
- Zafriou, O. C., & Bonneau, R. (1987). Wavelength-dependent quantum yield of $^{\bullet}\text{OH}$ radical formation from photolysis of nitrite ion in water. *Photochemistry and photobiology*, 45(S1), 723–727.
- Zafriou, O. C., Jousset-Dubien, J., Zepp, R. G., & Zika, R. G. (1984). Photochemistry of natural waters. *Environmental Science & Technology*, 18(12), 358A–371A.
- Zafriou, O. C., & True, M. B. (1979a). Nitrate photolysis in seawater by sunlight. *Marine Chemistry*, 8(1), 33–42.
- Zafriou, O. C., & True, M. B. (1979b). Nitrite photolysis in seawater by sunlight. *Marine Chemistry*, 8(1), 9–32.
- Zahnle, K. J., Gacesa, M., & Catling, D. C. (2018, September). Strange messenger: A new history of hydrogen on Earth, as told by Xenon. *ArXiv e-prints*.
- Zehr, J. P., & Ward, B. B. (2002). Nitrogen cycling in the ocean: new perspectives on processes and paradigms. *Applied and Environmental Microbiology*, 68(3), 1015–1024.
- Zellner, R., Exner, M., & Herrmann, H. (1990). Absolute $^{\bullet}\text{OH}$ quantum yields in the laser photolysis of nitrate, nitrite and dissolved H_2O_2 at 308 and 351 nm in the temperature range 278–353 K. *Journal of Atmospheric Chemistry*, 10(4), 411–425.
- Zerkle, A., & Mikhail, S. (2017). The geobiological nitrogen cycle: From microbes to the mantle. *Geobiology*, 15(3), 343–352.
- Zheng, X.-Y., Beard, B. L., Roden, E. E., Czaja, A. D., & Johnson, C. M. (2018). New constraints on ferrous Fe concentrations in the Archean ocean. In *Goldschmidt abstracts* (p. 3033).
- Zhu, I., & Getting, T. (2012). A review of nitrate reduction using inorganic materials. *Environmental Technology Reviews*, 1(1), 46–58.